Journal Pre-proof

Assessment of different combinations of substrate-filter membrane in green roofs

Diego Carrera, Ignacio Lombillo, Jaime Carpio-García, Haydee Blanco

PII: S2352-7102(21)01313-9

DOI: https://doi.org/10.1016/j.jobe.2021.103455

Reference: JOBE 103455

To appear in: *Journal of Building Engineering*

Received Date: 27 August 2021

Revised Date: 1 October 2021

Accepted Date: 11 October 2021

ASSESSMENT OF DIFFERENT COMBINATIONS OF SUBSTRATE-FILTER MEMBRANE IN GREEN ROOFS

Diego Carrera[a], Ignacio Lombillo[b*], Jaime Carpio-García[c], Haydee Blanco[b]

[a] University of Cantabria, Civil Engineering School, Santander, 39005, Spain

[b] Dept. of Structural and Mechanical Engineering, University of Cantabria, Civil Engineering School, Santander, 39005, Spain

[c] GITECO Research Group, University of Cantabria, Civil Engineering School, Santander, 39005, Spain

Author Statement

The contributions from each author to this paper have been listed below. **Diego Carrera**: Investigation, Formal analysis, Data Curation. **Ignacio Lombillo**: Conceptualization, Methodology, Validation, Resources, Writing - Review & Editing, Supervision. **Jaime Carpio-García**: Conceptualization, Methodology, Validation, Resources, Writing - Review & Editing. **Haydee Blanco**: Formal analysis, Visualization, Writing - Original Draft

Assessment of different combinations of substrate-filter membrane in green roofs

OBJECTIVE

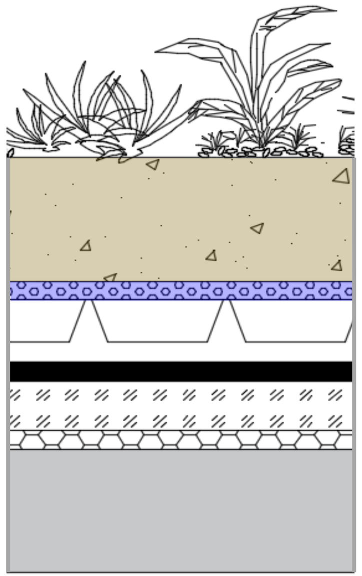

MATERIALS

9 composite sections: S_iG_j

INDICATORS

Indicator	Units	Substrate	Geotextile	Composite Section
Life cycle cost	€/m^2	X	X	
Carbon footprint	kg CO_2 eq./m^2	X	X	
Organic matter composition	% in weight	X		
Thermal insulation (U)	W/m^2·K	X		
Density				
bulk	kg/m^3			X
saturated				X
Permeability	l/m^2·s		X	X
Effluent organic matter content	mg/l			X
Static puncturing	kN		X	
Dynamic perforation	mm		X	
Characteristic opening	mm		X	
Mass per unit surface area	kg/m^2		X	
Hydrolysis resistance			X	
Oxidation resistance			X	

ELIGIBILITY

Multi-Criteria Decision Analysis (MCDA)

ELECTRE method

Substrate:

(S2 > S1) >> S3

Filtering layer:

(G2 >> G1) > G3

Composite section:

(S2G1 > S2G2) >> S1G2 >> S2G3 >> S1G1 >> (S3G2 > S3G1 > S3G3) >> S1G3

CONCLUSION: A methodology to evaluate the substrate layer and the geotextile was designed. Three types of substrates and three geotextiles were analysed. Geotextiles and substrates were combined and nine composite sections were studied. The list of indicators was based on the three pillars of sustainability. Among other solutions, a novel one, based on recycled phenolic foam, was studied. Composite sections including reused or recycled material show higher performance.

Journal of Building Engineering

D. Carrera, I. Lombillo, J. Carpio-García, H. Blanco (2021)

ASSESSMENT OF DIFFERENT COMBINATIONS OF SUBSTRATE-FILTER MEMBRANE IN GREEN ROOFS

Diego Carrera[a], Ignacio Lombillo[b*], Jaime Carpio-García[c], Haydee Blanco[b]

[a] University of Cantabria, Civil Engineering School, Santander, 39005, Spain

[b] Dept. of Structural and Mechanical Engineering, University of Cantabria, Civil Engineering School, Santander, 39005, Spain

[c] GITECO Research Group, University of Cantabria, Civil Engineering School, Santander, 39005, Spain

* Corresponding author

Abstract

Many strategies focus on supporting green infrastructure as a mechanism to contribute to economic growth while safeguarding the environment. However, the effectiveness and performance of green roofs depend on the composition and properties of layers, and their interaction, which has received little attention. Therefore, the article aims to establish the suitability of nine different combinations of substrate-geotextile (filter membrane) in green roofs. This study is novel as it introduces the global performance of different green roof configurations, including: common material frequently used in green roof applications (1), recycled or reused material (2), and proposals for novel materials (3) for which there was no evidence of recurrent use in this field. For this purpose, a multi-criteria decision analysis is developed considering several key indicators selected under sustainability criteria. To carry out this analysis, the indicators were experimentally quantified through laboratory tests, while the importance given to each indicator was evaluated through bibliographic references and consultation with experts in the sector. Results showed that the substrate including reused or recycled material (S2) generally provides better performance, and highlighted the suitability of combinations with both woven polypropylene geotextile (G1) and non-woven geotextile made using recycled polypropylene (G2).

Keywords

Green roofs; Substrate; Filter membrane; Geotextile; Sustainability assessment.

1. Introduction

Traditionally, horizontal surfaces in cities have been composed of two basic typologies: roofs and pavements. These surfaces severely waterproof the soil, reducing infiltration, eliminating natural vegetation and thus reducing rainwater interception and evapotranspiration [1]. In addition to the effects on the water cycle, cities, because they have very low albedo, reflect a very small proportion of the solar radiation that falls on their surface, absorbing it and producing what is known as the 'heat island' effect [2-4], which generates the consequent warming of the cities [5,6]. This leads to increases in energy consumption and greenhouse gas emissions, with the resultant increase in pollution [7], turning the city into a nucleus of worsening environmental quality. In this way, buildings account for 40% of total energy consumption worldwide [8] and 36% of European greenhouse gas emissions [9] influencing the resilience of cities to alterations in temperature, water-related processes, energy and air quality [10]. Green roofs can contribute to combating these issues by promoting economic growth and safeguarding environmental and human wellbeing [11,12].

Nowadays, the use of green roofs has rapidly spread around the world thanks to the significant advantages they have over traditional roofs, and to increasing social awareness. Human experiences of their use are increasingly positive, with continuous development of technology and study of materials and processes [13,14], which have led to lower execution and maintenance costs, in addition to lightening the weight of roof sections. In Germany, the promotion of green roof construction led to the fact that, at the beginning of the 21st century, more than 10% of all buildings were built with this type of roof, with an annual increase in the volume of the green roof industry of 10 to 15% [15]. In Spain, cities such as Barcelona earmark part of their municipal budgets to partially finance projects for the vegetation of building roofs [16]. In this sense, Japan has indicated that green roofs constitute key technology to reduce the urban heat island and promote sustainable buildings [17]. For example, in Tokyo there is a municipal ordinance that requires buildings with a floor area greater than 1000 m^2 to implement a vegetated roof [18]. Regarding North America, the analysis of the green roof industry indicates an estimated 5-15% overall growth trend in the period 2013-2018, although this is a conservative estimate [19].

In green roofs (**Figure 1**), the substrate layer is crucial for the supply of nutrients, water and oxygen to the supporting plant cover. Its thickness is directly related to the plant species it will contain [20], as well as to the climatic conditions to which it will be exposed throughout its useful life (mainly evapotranspiration). Generally, the density of the saturated substrate should not exceed 1300-1400 kg/m^3 [21], which should be sufficient to resist erosion, especially if the location is characterized by high wind intensity and/or the roof is sloped. NTJ-11E [22] and NTJ-11I [23] contain a series of recommended values for extensive and intensive roofs, respectively, related to granulometry, density, air content, pH, organic matter, among others. As for the insulating potential of the substrate layer, it is necessary to relate it to the climate to which the building will be subjected. Thus, in cold climates, it saves between 20 and 60% of the energy consumption for heating the building, while in warm-temperate climates its insulating power saves up to 75% of the energy used to keep the rooms cool [24]. This shows the importance of adopting sufficient substrate thickness, otherwise a thermal insulation layer must be installed. In addition, the behaviour of the substrate with respect to the outside temperature is non-linear, i.e., the more extreme the temperature, the more effective the substrate layer will be in terms of thermal insulation; however, its effect is influenced by atmospheric precipitation, making it necessary to study different typologies and materials for each specific location [25].

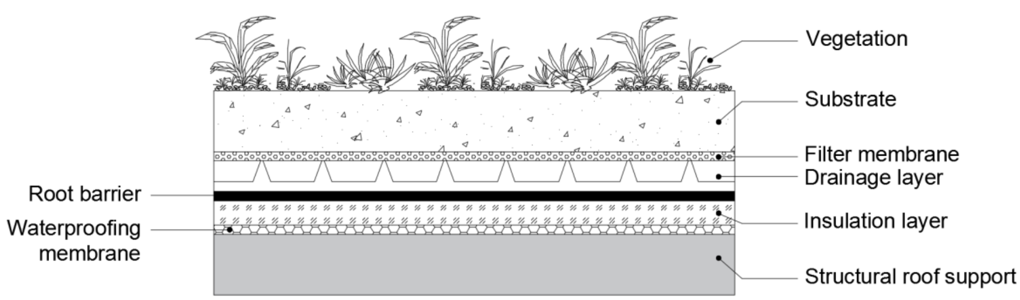

Figure 1. Schematic of the usual structure of a vegetated roof.

Generally, a draining layer is placed under the substrate. It plays an important role not only to eliminate excess water in the case of heavy rainfall, but also to store water in the case of dry places or periods;

nevertheless, in some cases, draining layers are not included where very permeable substrates or steep roofs are used. Of course, drainage must be ensured in critical conditions, associated with situations of continuous heavy rainfall. To avoid problems that would diminish the performance of the substrate and the drainage layer, it is usual to place a separating filter layer between them. Its function is to block the passage of fines from the upper layer, preventing them from being washed away and consequently clogging the drainage layer. In extensive roofs, this filtering layer, composed of a sheet made of synthetic fibres (geotextile) [26], should be laid over the entire surface of the drainage layer, with minimum overlaps of 10 cm between adjacent sheets [22].

Geotextiles are an essential part of vegetated roofs even though their thickness represents a very small part of the total system. Their development since the 60s [27] opened the door to the remarkable improvement in the properties of green roofs, their use being remarkable since the 80s [28], thus considerably increasing the potential of this type of construction. There is still significant room for development, especially with the use of new materials. The geotextiles used in green roofs must provide a series of characteristics that make them resistant to stresses during their installation and subsequent useful life, without penalizing the hydraulic conditions of the system as a whole. Thus, the permeability must be adequate to allow sufficient water to circulate towards the drainage layer and the filtering function must be effective, avoiding clogging by fines migrating from the substrate carried by the infiltration water. The materials most commonly used in the manufacture of geotextiles are polyethylene and polypropylene, due to their excellent mechanical properties and high durability under conditions of hydrolysis, oxidation and attack by microorganisms [29-31]. In addition to the above properties, both materials can be reused or made from recycled material after a pellet manufacturing process, thus significantly reducing the carbon footprint by no longer extracting fossil-based components.

Therefore, the planning of these elements provides a multifaceted opportunity to help to fulfil some of the United Nations Sustainable Development Goals (SDGs) [32], which seek to protect the planet and ensure prosperity for all [33]. In this way, the low embodied carbon and energy associated with green roofs [34], as well as the use of recycled materials in the substrate layer [35-37], are relevant to SDGs which deal with the effects of resource efficiency on energy and environment (SDG7-target 7.3; SDG11-targets 11.3/11b/11c; and SDG12-targets 12.1/12.5/12a). Green roofs have undoubted advantages in relation to other roof typologies in terms of runoff [38,39], pollution [40] and temperature reduction [41], which are concepts extremely closely linked to water-related issues (SDG6-targets 6.3/6.6), contamination (SDG3-target 3.9; SDG11-target 11.6), and climate-related hazards and natural disasters (SDG1-target 1.5; SDG11-target 11b; SDG13-targets 13.1/13.2; SDG15-target 15.3). Moreover, green roofs also have more potential than others to support the presence of animal and plant species and the growth of crops, which enable several targets to be met in achieving sustainable food production (SDG2-target 2.4), strengthening social and environmental links between urban, peri-urban and rural areas (SDG11-target 11.a) and ensuring the conservation / restoration / sustainable use of terrestrial urban ecosystems (SDG15-target 15.1). Finally, regarding thermal and acoustic insulation [42], green roofs have good performance, these topics being associated with SDG7-target 7.3 and SDG11-targets 11.3/11.7, concerning the safeguarding of the energy efficiency and adequate behaviour of buildings.

In general, experimental studies are usually limited by the specific green roof configurations and local climatic settings. As a result, studying the performance of green roofs is becoming increasingly important. Cascone et al. [43] analysed different substrate-vegetation configurations to assess thermal performance and to provide information on vegetation and substrate layer design. The study was carried out based on realistic literature values drawn from previous experimental tests. Additionally, simulations carried out in EnergyPlus allowed the authors to conclude that some configurations had better performance throughout the year in a Mediterranean climate. Moreover, it was found that the performance of extensive green roofs depended largely on the thermophysical properties of the substrate used. Regarding substrate mixture, Eksi et al. [44] suggested that the addition of 60 or 80% compost resulted in the greatest plant growth and fruit yields.

Other authors have conducted complete Life Cycle assessment of permeable pavements [45] or green roofs [46], demonstrating that these structures are efficient and contribute to sustainability and energy saving in civil construction and buildings.

Other studies have analysed the thermal behaviour of green roofs [24,47,48]. Based on the current literature, the energy-related performance of green roofs is still the most common benefit for which they are adopted [49]. Even though examples of experimental analysis can be found in the literature, most of the studies that quantify the achievable energy savings are based on numerical simulations [50]. Some experimental studies [51-53] have shown results in terms of heat fluxes through the building roof measured onsite. In this sense, the influence of substrate depth and vegetation type have been investigated in an experimental study conducted on a green roof of the Michigan State University [54]. For this purpose, the green roof sections were fully fitted with instrumentation to measure heat flux, temperature and moisture. Results demonstrated that herbaceous plants were able to provide greater thermal protection, with more stable temperature fluctuations and heat flux under the vegetation layer. Similar research focused on energy-related topics was performed in [55,56]. Despite the relevant amount of research on green roofs existing in the literature, there is no straightforward answer to the question of how much energy a green roof can save [11], because the climatic conditions and design (substrate, plants, etc.) are the main factors affecting performance.

Consequently, this study proposes to assess the suitability of different configurations of substrate layer and geotextile (separating layer) of green roofs. To this end, the study focuses on analysing three types of substrates and three geotextiles, as well as their nine possible combinations. The materials used included a common material frequently used in vegetative roof applications, a recycled or reused material, and a novel material for which there was no evidence of frequent use in this field. The global performance is also compared through a Multi-Criteria Decision Analysis (MCDA) based on the ELECTRE method. For this purpose, a series of indicators were selected to meet sustainability criteria. The objective of the method is not to analyse the performance of a given material in relation to an individual parameter, but to evaluate its overall behaviour in relation to all of them, and in comparison with other existing alternatives. Thus, a comprehensive ranking is proposed to identify which substrate-geotextile combinations offered the highest global performance, considering all of the selected indicators. These results will provide information regarding responses of several green roof configurations.

2. Materials and methods

2.1. Multi-Criteria Decision Analysis (MCDA)

Several multi-criteria analysis methods have been prominently used in the construction field [57], the Electre method being one of the most widely used. This method began its development in 1968 [58], and to date has been updated in different versions [59]. One of the fundamental advantages is that, through the application of the concordance and discordance matrices, it is relatively easy to discard alternatives and restrict their number to a more manageable level in cases where the set of starting alternatives greatly penalizes the study time.

The application process includes [60]:

1. Definition of the criteria to be used to evaluate the suitability of the alternatives, in this case based on the principles of economy, environment and society.
2. Grading of the criteria, assigning entire values from 1 to 10 according to their importance (weight).
3. Assessment, one by one, of the different alternatives according to each of the defined criteria, being collected together with the weights in the 'Matrix of weights and ratings'. They must be graded by whole numbers from 1 to 10. The most advantageous alternative will receive the highest score.
4. Calculation of concordance and discordance matrices, and prioritization of alternatives.

2.1.1. Definition of the indicators

The most important criteria to be taken into account are based on the three fundamental pillars of sustainability (economy, environment and society), based on those established by MITMA [61]. When studying the substrate and geotextile layers, it became necessary to adapt these criteria to a series of factors that could be measured during the experimental campaign. Consequently, the best substrate-geotextile composition was selected from the point of view of sustainability and resilience of current-future cities.

For this purpose, a preliminary list of indicators based on the TBL (Triple Bottom Line, [62]) was drawn up, **Table 1**. In order to obtain an objective assessment of the relevance of the pre-selected indicators, including their weights in the multi-criteria analysis, external professionals with extensive and proven experience in green roofs and building, planning and management of urban spaces and/or energy efficiency were consulted. Four levels of importance were established (Very Important, Important, Slightly Important and Not Important). A total of 43 experts were consulted, who work in municipalities, industry, research and academia. Only 10 experts responded, mainly from academia, technology research and the construction industry. Moreover, as all respondents are architects/engineers in constant contact with public administrations, the surveys received were considered representative, although a larger number of experts and perspectives would be desirable. Based on the results of the surveys, an index was created, consisting of the normalization of the degrees of importance with respect to the total number of responses received, giving the following weights, the values of which are shown in **Table 1**.

- Very Important (VI): 4 points
- Important (I): 3 points
- Slightly Important (SI): 2 points
- Not Important (NI): 1 point

Considering the levels of importance given by the experts, once normalized, the level of importance corresponding to each indicator was obtained as a result. These are listed in **Table 2** from highest to lowest rating. In addition to the weights given by the experts to each of the indicators mentioned above, they proposed new indicators, of which *'Compaction'* was added, applied to the study of the composite section.

Table 1. Proposed indicators and levels of importance.

Indicator	Components				Standardization of surveys					
	Units	Substrate	Geotextile	Composite Section	Nº of experts				∑ (Imp weight)	Normalized
					VI	I	SI	NI		
Life cycle cost	€/m^2	X	X		6	2	1	1	33	3.30
Carbon footprint	kg CO_2 eq./m^2	X	X		1	6	2	1	27	2.70
Organic matter composition	% in weight	X			2	4	3	1	27	2.70
Thermal insulation (U)	W/m²·K	X			4	4	0	2	30	3.00
Density										
bulk	kg/m^3			X	2	5	3	0	29	2.90
saturated				X						
Permeability	l/m^2·s		X	X	7	2	1	0	36	3.60
Effluent organic matter content	mg/l			X	2	2	6	0	26	2.60
Static puncturing	kN		X		5	2	3	0	32	3.20
Dynamic perforation	mm		X		5	3	2	0	33	3.30
Characteristic opening	mm		X		3	3	4	0	29	2.90
Mass per unit surface area	kg/m^2		X		0	4	6	0	24	2.40
Hydrolysis resistance			X		1	8	1	0	30	3.00
Oxidation resistance			X		1	8	1	0	30	3.00

Table 2. Summary of the importance of the indicators.

Indicator	Normalized	Importance
Permeability	3.60	Very important - Important
Life cycle cost	3.30	Important - Very important
Dynamic perforation	3.30	Important - Very important
Static puncturing	3.20	Important - Very important
Thermal insulation (U)	3.00	Important
Hydrolysis resistance	3.00	Important
Oxidation resistance	3.00	Important
Density	2.90	Important - Slightly important
Characteristic opening	2.90	Important - Slightly important
Carbon footprint	2.70	Important - Slightly important
Organic matter composition	2.70	Important - Slightly important
Effluent organic matter content	2.60	Important - Slightly important
Mass per unit surface area	2.40	Slightly important - Important

2.1.2. Criteria for ELECTRE Method

Based on the selected sustainability criteria, 4 indicators were used for the substrates, 9 for the filtering separator layer and 5 for the composite sections (substrate + filtering separator layer). In each case, weights were established from 1 to the number of indicators adopted, in increasing order of relevance (**Table 3**).

Table 3. Weights assigned to the indicators adopted to evaluate each component.

Component	Indicator	Weight
Substrate	Life cycle cost	4
	Thermal insulation (U)	3
	Carbon footprint	2
	Organic matter (OM) composition	1
Filtering separating layer	Permeability	9
	Life cycle cost	8
	Dynamic perforation	7
	Static puncturing	6
	Oxidation resistance	5
	Hydrolysis resistance	4
	Carbon footprint	3
	Characteristic opening	2
	Mass per unit surface area	1
Composite section (substrate + filtering separating layer)	Permeability	5
	Density	
	saturated	4
	bulk	3
	Compaction	2
	Effluent organic matter (OM) content	1

Thus, considering the order of the indicators obtained from the consultation with external experts, **Table 2**, in the case of substrates, the highest weight was given to *Life Cycle Cost*, followed by *Thermal Insulation*, with *Carbon Footprint* and *Organic Matter (OM) Composition* having lower weights.

In the case of the indicators referring to geotextiles, *Permeability* is the fundamental parameter due to its relevance in draining precipitation quickly or reducing peak flows, depending on the need. Similarly to what happens with substrates, *Life Cycle Cost* is one of the main indicators, obtaining the second highest weight due to its great relevance in terms of sustainability. This is followed by the resistance criteria to *Dynamic Perforation* and *Static Puncturing* as they are directly linked to the mechanical integrity of the geosynthetic and, therefore, its functionality. This is followed by *Oxidation* and *Hydrolysis Resistance,* as the maintenance of their qualities will dictate their long-term hydraulic and filter performance. Finally, the criteria of least relevance are the *Carbon Footprint*, the *Characteristic Opening* and the *Mass per unit surface area*, because, although important, variations in their magnitudes will affect the sustainability and performance of the system to a lesser extent.

Finally, for the composite section, *Permeability* represents the most relevant indicator due to its effect on draining or laminating precipitation, as the case may be. It is followed by *Density*, more relevant in the saturated state than apparent (measured in the state of reception of materials) due to its relationship with the availability of water (cistern effect) for the vegetation cover and due to the effect of increasing weight for the overall roof structure once the precipitation phenomenon is over. *Compaction* received a weighting of 2, since excessive compaction of the substrate used can in the most extreme cases nullify plant growth, followed by the *OM content of the effluent* in last place, since a very rapid loss of mineral components in the form of dissolution can also impair plant growth.

2.2. Materials and methods

2.2.1. Description of materials

The development of the experimental campaign contemplated the use of 3 types of substrate and 3 geotextiles, considering the following criteria for their selection:

- A common component or material frequently used in the bibliography consulted and in the catalogues of different manufacturers.
- An element composed of recycled components whose recycling and transport process would not imply high levels of energy, financial cost or contaminant emissions, with the aim of seeking options that are as sustainable as possible.

- A novel material, with no or very limited use on a global scale in this type of roofing, in order to verify its suitability for the established indicators and measure its impact on the parameters produced by the system.

As for substrates, three compounds were used. First, a coarse-grained inert material (gravel, recycled coarse stone aggregate or recycled and crushed coarse ceramic aggregate) was used. Its main function is to enable the maintenance of aeration inside the substrate and to prevent the substrate from caking. Second, an inert material of smaller diameter such as silica sand or perlite was utilised, which collaborates in the fixation of pollutants and is integrated with the third component, an organic by-product (peat, topsoil, compost, etc.).

As a novel solution, the use of recycled phenolic construction foam was proposed as a component of the substrate. This material is mainly used for thermal insulation of pavements, but it has already been successfully used in plant production studies during the first decade of the 21st century [63]. The addition of geofoam was intended to buffer infiltration from atmospheric precipitation more effectively and to facilitate the generation of a water reserve for the vegetation cover.

In order to reduce the variability of the components of the substrates, the same compost was chosen for the organic portion of all three substrates, and with the same dosage (one third in volume of the mixture). Thus, the analysis of the response of the samples would focus on the influence of the other components (mineral fraction and phenolic foam), since they have a greater impact on the behaviour of the system, especially in hydraulic terms.

Thus, the proposed compositions of the 3 substrates formed from the above-mentioned compounds were as follows (**Figure 2**):

- CLASSIC (S1): Limestone gravel ($\%_{volume}/3$) + Silica sand ($\%_{volume}/3$) + Compost ($\%_{volume}/3$)
- RECYCLED (S2): Crushed brick ($\%_{volume}/3$) + Silica sand ($\%_{volume}/3$) + Compost ($\%_{volume}/3$)
- NOVEL (S3): Crushed brick ($\%_{volume}/5$) + Silica sand ($\%_{volume}\cdot 4/15$) + Phenolic foam ($\%_{volume}/5$) + Compost ($\%_{volume}/3$).

The determination of the optimal quantity of recycled or novel components of the substrate was not considered at this point by the authors. This study will be carried out as part of future research, in which statistical tools such as DOE (design of experiments) could be used.

Figure 2. Appearance of the materials in their original state.

Figure 3 illustrates the final appearance of the three proposed substrate configurations.

Figure 3. Appearance of substrate mixtures.

As for the geotextiles, 3 options were also proposed, which are described below (**Figure 4**):

- CLASSIC (G1): Geocomposite with a mass per unit area of approximately 250 g/m^2 consisting of black woven polypropylene (PP) geotextile bonded to green non-woven geotextile with 70% polypropylene (PP) and 30% polyethylene (PE).
- RECYCLED (G2): Reused white polypropylene (PP) non-woven geotextile, with a mass per unit area of approximately 250 g/m^2.

- NOVEL (G3): Expanded polystyrene geofoam (EPS) with a mass per unit volume of approximately 22 kg/m^3.

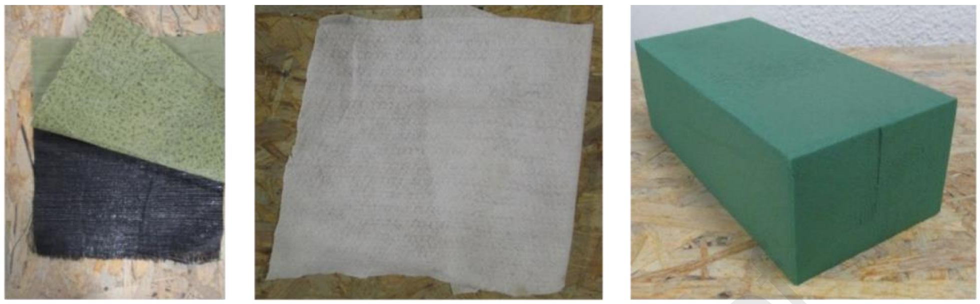

Figure 4. Appearance of the geosynthetics used in their original state.

The first two have a consolidated background in both construction and gardening [64-66], providing remarkable performance and presenting good behaviour in most applications. The third material considered, geofoam, has particular qualities that make it attractive for use in vegetated roofs [67] as well as in Sustainable Urban Drainage Systems (SuDS). Its porosity and permeability enable high water storage, around 95-97% of its volume [68], which provides moisture retention that provides the covering with considerable reserves when confronting seasons without rainfall. It is not widely used due to the still limited knowledge about its behaviour in this field of construction, so this is an attractive opportunity to provide knowledge about its performance and the benefits the material can provide to green roofs.

Finally, the 3 types of geotextile were combined with the three substrate configurations to produce a total of 9 composite sections (S_iG_i).

2.2.2. Methods for quantification of indicators

The tests carried out on the substrates, geotextiles and composite sections were aimed at evaluating each of the previously selected indicators. The following is a description of each of the methods used for their quantification.

2.2.2.1. Substrates

The first of the parameters evaluated corresponded to the *Life Cycle Cost* study, which includes the costs induced by the production of materials, construction, maintenance and demolition of the element. In this case, the functional unit selected was the price per unit area (€/m^2) and the analysis period was 100 years. For the estimation of this indicator, GaBi 9.1 software, created by Thinkstep, an international benchmark for the calculation of Life Cycle Cost and Carbon Footprint, was used. Similarly, the CYPE price database [69] was used to extract the costs associated with installation and maintenance.

The *Carbon Footprint* analysis was carried out according to UNE-EN ISO 14044 [70]. This is the total emissions generated by a product from the extraction of its raw materials to its end of life, expressed in units of mass of carbon dioxide equivalent per unit area for this particular case (kg CO_2 eq. /m^2), over an estimated period of 100 years.

In order to evaluate the *OM Content* of the substrates, the procedure described in the 2540 SOLIDS standard [71] was followed. Porcelain containers were used to prevent the material from adhering to the walls of the container. After a previous acclimatization process by keeping the samples for 24 hours at a constant temperature of 104 ºC, they were calcined at 550 ºC and the difference in masses was measured.

In addition, in order to evaluate the *thermal insulation* provided by the substrate layer of each of the samples, and due to the lack of the necessary equipment to carry out the tests in accordance with UNE-EN ISO 6946 [72], an evaluation was made based on the consultation of bibliographic sources. The method used establishes how to obtain the thermal resistance of each homogeneous part of the component, combining the individual resistances to obtain the total thermal resistance of the component. From this value the thermal transmittance (U) was obtained.

2.2.2.2. Filtering separating layer (geotextile)

The tests on the geotextiles began with the conditioning of the samples under conditions of temperature and relative humidity of 20 ± 2 ºC and 65 ± 5 %, respectively (**Figure 5a**), according to ISO 554 [73]. Next, the *Life-Cycle Cost* and *Carbon Footprint* were studied, following the same procedure as for the substrate samples.

Permeability of geotextiles was measured according to UNE-EN ISO 11058 [74], see **Figure 5b**. In this test, a unidirectional flow of water is made to circulate perpendicularly to the plane of the geotextile forming part of the specimen using a decreasing variable load height, thus taking into account the heterogeneity of water conditions on the roof.

The determination of the *Static Puncturing r*esistance was carried out in accordance with the UNE-EN ISO 12236 [75]. For this purpose, a point force was applied through a punch with a flat end, recording the force required to pass through the geosynthetic. The punch used was made of stainless steel with a diameter of 50 ± 0.5 mm and an angle of attack radius of 2.5 ± 0.2 mm. The test was performed on dry specimens clamped between two steel rings, allowing the metal plunger to advance perpendicularly towards the specimen at a constant speed (**Figure 5c**). It should be noted that in the case of geofoam, the test was not carried out due to the fragility of the material.

The *Dynamic Perforation* test is associated with the possibility of the geotextile being affected by falling angular stones or other sharp objects during the installation of the construction. The test was performed by measuring the resistance of the geotextiles to the penetration of a steel cone in free fall, according to UNE-EN ISO 13433 [76]. The stainless-steel cone, with a tip angle of 45° and smooth and polished surface, with a mass of 1000 ± 5 g, was placed at a height of 500 mm for dropping. The product behaviour is estimated through the measurement of the diameter of the hole generated. **Figure 5d** illustrates the test machine used in the experimental campaign. As in the previous case, the test was not carried out in geofoam due to the fragility of the material itself.

Another parameter determined was the *Characteristic Opening* size measurement, which is oriented to determining the pore size measurement of an individual geotextile layer, applying the principle of wet sieving. The test was carried out following the procedure described in UNE-EN ISO 12956 [77]. The characteristic opening is defined as 90% of the maximum aggregate size passing through the geotextile. This size is obtained by strict filtration of the effluent water (**Figure 5e**).

The next indicator evaluated was *Hydrolysis Resistance*. The test for its determination, defined in UNE-EN ISO 12447 [78], establishes the resistance of a geotextile to hydrolysis, through the exposure of specimens submerged in type 3 deionized water at 95ºC, after which the changes in properties undergone during exposure are evaluated. The objective of its determination was to establish a minimum acceptable durability of the component. **Figure 5f** shows the general arrangement of the specimens inside the vessel.

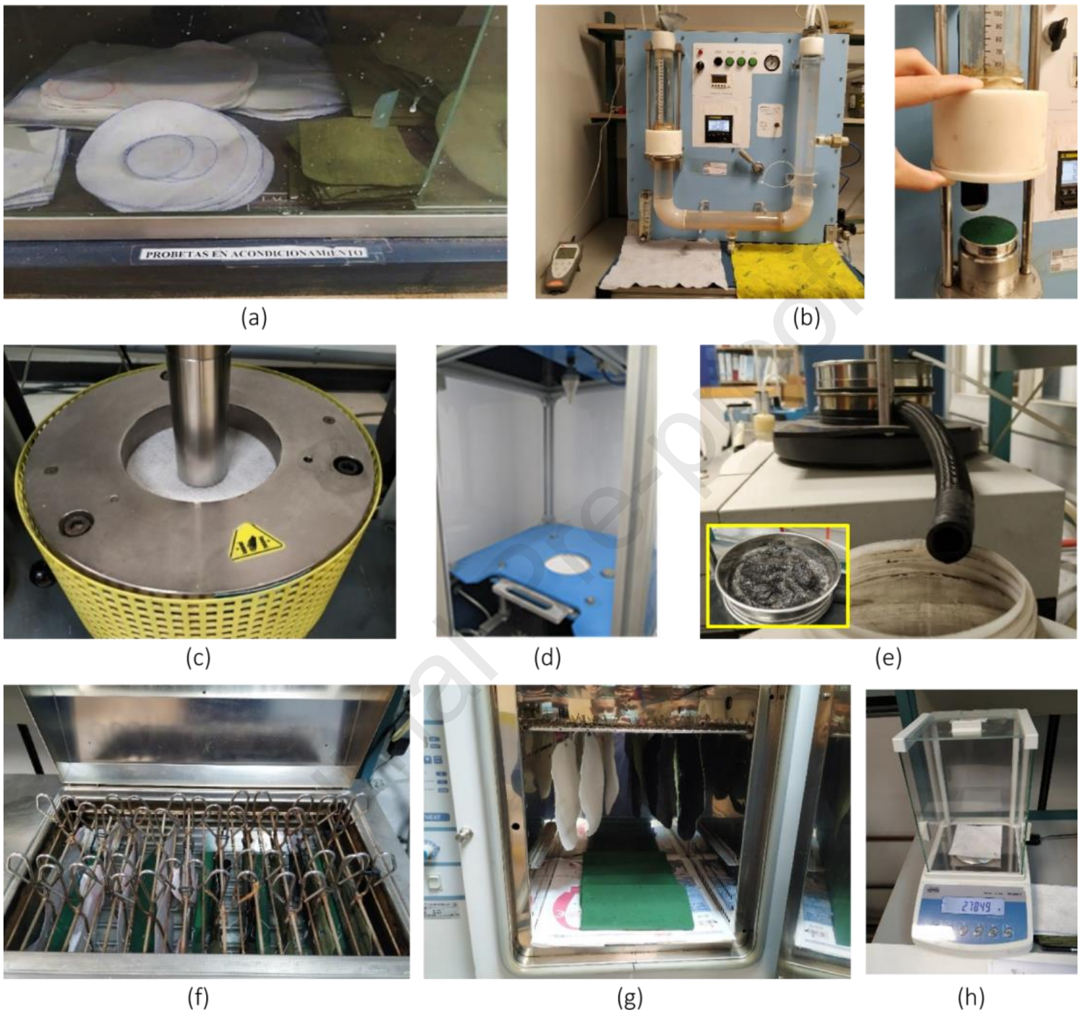

Figure 5. Main tests performed on geotextiles: (a) conditioning of specimens, (b) perpendicular to plane permeability test, (c) static puncturing test, (d) specimen tested against dynamic perforation, (e) characteristic opening test, (f) arrangement of submerged specimens in hydrolysis resistance test, (g) thermal exposure of specimens during oxidation resistance test, and (h) weighing of specimens during determination of mass per unit surface area.

Regarding the analysis of the *Oxidation Resistance* of the samples, it should be noted that they were stored in grade 3 water (distilled) for 28 days prior to the test, and then exposed to air for another 28 days (time established by the standard to evaluate 25 years of useful life) at a temperature of 100 ± 1 ºC, **Figure 5g**. After the aging period, the specimens were subjected to in-plane permeability and characteristic opening tests, instead of the tension test described by UNE-EN ISO 13438 [79], since these were considered more appropriate tests to evaluate the aging of geosynthetics.

Finally, in order to facilitate the identification of geotextiles and their potential use in civil works, the *Mass per unit surface area* indicator was quantified. This parameter was calculated by weighing specimens of nominal size of 100 cm^2 (**Figure 5h**), according to UNE-EN ISO 9864 [80].

2.2.2.3. Composite section (substrate + filtering separating layer)

The study of the composite section was carried out through the analysis of 5 indicators. The first one corresponded to the *Bulk Density*, determining the density of the substrate samples tested together with the geotextile. For this purpose, the product was weighed in reception conditions, not strictly dry, since the conditions were representative of its installation on site. In addition, the *Density in saturated state* was determined after performing the saturation flow test, which is explained below.

For the *saturation flow* study, it was necessary to design an ad hoc test device (**Figure 6**) since it was a composite section in which the substrate had to present a thickness representative of a possible real arrangement. The test was initiated by adding water in a uniformly distributed manner over the 30x30 cm test surface. Initially, a flow rate of 30 l/h (330 mm/h approximately) was established until water began to drip through the geotextile. Then, the flow rate was increased to 40 l/h (440 mm/h), taking a sample of the water emanating in less than 5 minutes, which would be used to measure the *OM Content* indicator of the effluent as indicated in the following paragraph. The flow rate was then progressively increased at 5-minute intervals until the substrate was saturated, at which point a thin layer of water accumulated on the surface. At that moment, the hose was removed from the irrigation system and the circulating flow rate was measured in order to obtain the flow rate that floods the composite section

For the quantification of the pick *OM Content* of the effluent, the difference in masses between the acclimatized (24 hours at 104 ºC) and calcined (at 550 ºC) samples was measured, the difference corresponding to the organic matter present in the samples taken. The procedure was performed according to the 2540 SOLIDS standard [71]. The liquid sample was obtained in the initial part of the saturation flow study as indicated in the previous paragraph.

Figure 6. Test device designed ad hoc for the study of *Permeability*.

The last of the parameters evaluated corresponded to the measurement of *Compaction*. This indicator has a direct and simple measurement, which compares the change in thickness of the substrate layer tested, placed on the geotextile, before starting to pour water and once the saturation flow study test is completed.

3. Results and discussion

3.1. Quantification of indicators

3.1.1. Life cycle cost

From the price databases consulted in the GaBi 9.1 and CYPE software [69], unit prices and performance were obtained for materials, including the cost of raw materials, material production and transport up to manufacturing plant, as well as for the labour mobilized for the execution of the different sections of the study. These values are shown in **Table 4** and **Table 5**. To calculate the price per unit volume of the substrate mixtures, the unit price of each of its components was multiplied by the percentage by volume of each component in the mixture. In relation to the performance of geotextiles G1 and G2, a value of 1.10 was assigned to consider their adaptation to the geometry of the roof. In the case of geofoam (G3), a value of 1.20 was adopted due to its greater handling complexity, given its fragility, which implies greater material losses. In the case of substrates, instead of considering 0.15 m thickness per unit area, a reasonable value for extensive roofs [22] of 0.20 m was considered in order to take into account the compaction associated with the installation tasks on the roof.

Table 4. Unit price of materials.

Material	Unit	Unit price (€)
G1	€/m^2	1.00
G2	€/m^2	1.00
G3	€/m^3	30.00
Crushed brick	€/m^3	300.00
Topsoil (95% peatland+ 5% green compost)	€/m^3	80.00
Calcareous gravel	€/m^3	255.00
Silica sand	€/m^3	160.00
Geofoam for civil works and landfills	€/m^3	1000.00

Table 5. Prices and performance of materials and manpower per m^2 of green roof.

Unit	Material / Manpower	Performance	Unit price (€/ud.)
	Geotextile		
m^2	G1	1.100	1.00
m^2	G2	1.100	1.00
m^3	G3	1.200	30.00
h	Builder	0.109	19.46
h	Builder assistant	0.352	18.13
	Substrate		
m^3	S1	0.200	163.35
m^3	S2	0.200	178.20
m^3	S3	0.200	328.00
h	Gardener	0.841	19.46
h	Gardener assistant	0.841	18.55

In addition, calculations were made considering the substrate-geotextile combination. Thus, from the prices/performance of materials and labour, the cost of the work unit ‘Square meter of finished section (substrate-geotextile)' associated with each section was calculated (**Table 6**). It can be seen that the sections using geofoam (S_iG_3 and S_3G_i) have a higher unit cost.

Table 6. Cost of the work unit 'Square meter of finished section (substrate-geotextile)'.

Section	Cost (€/m²)	Section	Cost (€/m²)	Section	Cost (€/m²)
S1G1	74.24	S2G1	77.21	S3G1	107.17
S1G2	74.24	S2G2	77.21	S3G2	107.17
S1G3	109.14	S2G3	112.11	S3G3	142.07

Finally, the maintenance costs should also be considered in order to have an overall estimate of the life cycle cost of each of the sections. According to CYPE's price database, maintenance costs at current prices are estimated to be constant at around 104 €/m^2 every 10 years. However, due to the existence of geofoam in the S3 substrate and in the G3 separating layer, it was necessary to differentiate between the maintenance operations to be carried out in each section, since the geofoam has insufficient resistance to hydrolysis and oxidation processes, as will be discussed later, as well as very low resistance to static puncturing and dynamic perforation. Thus, the sections without geofoam in the substrate or in the separator layer (S1G1, S1G2, S2G1 and S2G2) will have a fixed routine maintenance cost of 104 €/m^2 every 10 years. Those sections with geofoam in the substrate, but not as a separating layer (S3G1 and S3G2) should contemplate 104 €/m^2 every 10 years as surface maintenance; to which lifting of the cover and replacement of the substrate every 20 years should be added, considering this action to be the maintenance cost plus the cost of the substrate material (65.6 €/m^2) and its new installation (31.97 €/m^2). On the other hand, in the sections with geofoam exclusively as a separating layer (S1G3 and S2G3), the lifting of the cover and replacement of the geofoam every 10 years should be considered, keeping the same substrate that should have adequately preserved its properties, considering the cost of maintenance (104 €/m^2), plus the cost of the geofoam (36.0 €/m^2) and its new installation (8.50 €/m^2). Finally, for the section that contemplates the provision of geofoam as part of the substrate and as a separating layer

(S3G3), a replacement of the separating layer every 10 years (148.50 €/m^2) should be considered, keeping the same substrate; and an additional replacement of the substrate (65.6 €/m^2 + 31.97 €/m^2), to be added to the previous cost, every 20 years.

Thus, and taking into account the analysis for a useful life of 100 years, **Table 7** shows that the use of geofoam increases the maintenance and, therefore, the life cycle cost at current prices, increasing by 37.53% when it is introduced as a component of the substrate (S3G1 and S3G2), by 42.79% when used as a separating layer (S1G3 and S2G3), and by 80.32% when used both in the substrate and in the separating layer (S3G3).

Table 7. Maintenance cost (€/m^2) at current prices of the different sections (substrate-geotextile) over 100 years.

Section	**Years**										**Total**
	10	**20**	**30**	**40**	**50**	**60**	**70**	**80**	**90**	**100**	**(€/m^2)**
S1G1, S1G2, S2G1, S2G2	104.00	104.00	104.00	104.00	104.00	104.00	104.00	104.00	104.00	104.00	1,040.00
S3G1, S3G2	104.00	201.57	104.00	201.57	104.00	201.57	104.00	201.57	104.00	104.00	1,430.28
S1G3, S2G3	148.50	148.50	148.50	148.50	148.50	148.50	148.50	148.50	148.50	148.50	1,485.00
S3G3	148.50	246.07	148.50	246.07	148.50	246.07	148.50	246.07	148.50	148.50	1,875.28

3.1.2. Carbon footprint

Like the life cycle cost, the carbon footprint was estimated using GaBi 9.1 software, which follows the CML methodology [81] for calculating impacts, based on ISO 14044 definitions. The analysis was performed for an equivalent unit area of 1 m^2 of each material. While production, including transport of raw materials, was considered, installation and maintenance were not taken into account. It was assumed that in the case of the geocomposite, both components were manufactured by the same manufacturer, so there was no additional impact of transporting one in relation to the other. The indicator was calculated per unit area in the case of both materials, taking as a reference a thickness of 5 cm for each of the components that made up the substrate mixtures (a total of 15 cm estimated thickness for the test, a usual thickness in practical applications).

As a summary, **Table 8** shows the values obtained for the Global Warming Potential (in kg CO_2 equivalent per m^2 for 100 years) for the manufacture of each geotextile and each type of substrate. The numbering of the materials forming the substrates is as follows:

- Material 1: topsoil or compost.
- Material 2: silica sand.
- Material 3: limestone aggregate.
- Material 4: crushed brick.
- Material 5: geofoam for civil works.

Table 8. Carbon footprint.

Component		Global Warming Potential (kg CO_2 eq. 100 years)
Geotextile	G1	6.15E-01
	G2	2.00E-01
	G3	6.45E-02
Substrate	S1 (1+2+3)	4.38E+00
	S2 (1+2+4)	3.51E+00
	S3 (1+2+4+5)	4.79E+00

It can be seen that substrate 3, which is more complicated to produce, has the highest carbon footprint, despite the fact that geofoam is the material with the lowest specific carbon footprint, since it is the lightest. In general, geotextiles have a lower carbon footprint than substrates.

3.1.3. Substrate OM composition

The organic matter concentrations obtained from the substrate are shown in **Table 9.** It can be observed that substrate sample S3 (Compost + Silica sand + Crushed brick + Geofoam) has the highest relative organic matter content. The presence of the geofoam, **Figure 7**, which differentiates this sample from the S2 substrate, produces a significant increase in the organic matter content (by weight % in dry sample), due to the lightness of this material.

Table 9. Results of the OM composition of the substrates.

Sample	OM (% by weight in dry sample)
S1	4.95
S2	3.55
S3	7.64

Figure 7. Samples prior to calcination.

3.1.4. Density

The bulk density of the substrate samples was determined before and after performing the permeability test. First, it was obtained in equilibrium under lab conditions ((20 ±2) ºC and (65% ± 5%) relative humidity). To calculate the volume of each sample, the average of the substrate heights on each of the four sides of the containment enclosure and the 30×30 cm plan area were considered. Then, after the permeability test, the substrate heights were measured again, thus calculating the saturated density of the material. The values recorded for both cases are illustrated in **Table 10**.

Table 10. Bulk density (in the received state) and saturated density of the substrates.

Substrate	Geotextile	Received density				Saturated density				Percentage variations in density (%)
		h_b (cm)	V_b (cm^3)	W_b (g)	D_b (kg/m^3)	h_s (cm)	V_s (cm^3)	W_s (g)	D_s (kg/m^3)	
S1	G1	12.88	11587.50	13189	1138.21	12.75	11475.00	17267	1504.75	32.20
	G2	12.50	11250.00	13040	1159.11	12.40	11160.00	14896	1334.77	15.15
	G3	12.75	10125.00	12855	1269.63	12.60	9990.00	12549	1256.16	-1.06
S2	G1	12.65	11385.00	11744	1031.53	12.58	11317.50	13956	1233.13	19.54
	G2	13.33	11992.50	12359	1030.56	13.10	11790.00	14759	1251.82	21.47
	G3	13.83	11092.50	11215	1011.04	13.78	11047.50	12853	1163.43	15.07
S3	G1	13.85	12465.00	9584	768.87	13.60	12240.00	12962	1058.99	37.73
	G2	14.38	12937.50	9485	733.14	13.88	12487.50	12633	1011.65	37.99
	G3	13.80	11070.00	7826	706.96	13.73	11002.50	10371	942.60	33.33

Under reception conditions
h_b: Height W_b: Weight
V_b: Volume D_b: Density

Under saturation conditions
h_s: Saturated height W_s: Saturated weight
V_s: Saturated volume D_s: Saturated density

If we analyse the geotextile in particular, the water retention recorded was generally higher for geotextile 1 than geotextile 3 (G1 > G2 > G3), with mean values of 29.83, 24.87 and 15.78%, respectively. It is curious that the use of geofoam as a separating layer shows a lower percentage variation in relation to the rest of the geotextiles. On the other hand, in the substrate, water retention was greater as compounds with greater water absorption capacity, such as crushed brick or geofoam (S1 < S2 < S3), were added. The mean values in this case corresponded to 15.43, 18.70 and 36.35% respectively.

The direct relationship between the properties of the materials contained in each type of substrate can be observed. When calcareous gravel (S1) was replaced by crushed brick (S2), the bulk density was reduced due to the lower density of the latter material (1000 kg/m^3 compared to 1400 kg/m^3 for gravel), despite having a smaller particle size that provided a lower percentage of voids in the mix. This makes it possible to reduce the weight of the roof and thus unload the slab structure supporting the green roof. In turn, the water retention capacity increased by approximately 8.8% thanks to the high relative retention capacity of the crushed brick, which is much more porous than gravel.

Likewise, by incorporating a portion of geofoam (S3) into this mixture (S2), the density was considerably reduced, by 28.1% in the case of the bulk density (in the as-received state) and by 17.4% in the case of the saturated one. This leads to a significant reduction in the loads. For the S3 substrate, the difference between dry and saturated densities is even more significant, increasing by 36.4%. This suggests a higher capacity to reduce peak rainfall flows and a high water retention capacity provided by the geofoam, which, despite the increase in weight under saturated conditions, enables the dry density to remain below the other two types of substrate tested.

3.1.5. Thermal insulation of substrates

As mentioned above, the thermal insulation of the substrates was obtained from bibliographic sources. These state that, in general, samples with higher density have a higher thermal conductivity [82], hence heavier substrates will provide less thermal insulation capacity to the system under dry conditions; maintaining conductivities between 0.1 W/m·K and 0.25 W/m·K [83]. Due to the provision of an equal proportion in volume of vegetable compost in each of the mixtures, this organic portion will not affect the thermal transmittance of the substrate, so that this property will depend on the rest of its constituent materials. Thus, and considering the densities obtained in the previous section, one would expect decreasing thermal transmittances from substrate S1 to S3. This would imply reaching a higher insulation capacity with the substrate containing geofoam (S3). To evaluate this incidence, substrate S3 was assigned the lowest conductivity mentioned above, with a value of 0.1 W/m·K, and substrate S1 the highest, with a value of 0.25 W/m·K; substrate S2 was assigned a value of 0.1955 W/m·K, obtained by linear regression from the initial average densities obtained in the reception state.

However, in the saturated state, the thermal transmittance varies. Due to the heterogeneity of the samples and the relatively dynamic state of the water within them [83], it is not possible to accurately evaluate this parameter, but it is possible to make a sufficiently accurate estimate. For this purpose, there are models that attempt to approximate the ratio of the thermal conductivity in the dry and saturated states of a substrate [84], as shown in the equation Eq. (1).

$$\frac{k_s}{k_{dry}} = \frac{\alpha \cdot \exp(\beta \cdot S_r)}{1 + (\alpha - 1) \cdot \exp(\beta \cdot S_r)} \qquad (1)$$

Where $\alpha = 1.45$; $\beta = 4.411$ and Sr is equal to the degree of saturation. Applying this equation to the estimated conductivity values results in conductivities in saturated state of 0.7844 W/m·K for S1, 0.6132 W/m·K for S2 and 0.3138 W/m·K for S3. These values are shown in **Table 11** and the thermal transmittance can be calculated from the equations Eq. (2) and Eq. (3).

$$U_s = \frac{1}{R_s} \qquad (2)$$

$$R_s = \frac{e}{k_s} \qquad (3)$$

U_s being the thermal transmittance in W/m^2·K, R_s the thermal resistance in m^2·K/W, k_s the thermal conductivity in W/m·K, all parameters in saturated state, where *e* is the thickness of the layer (15 cm).

Table 11. Estimated thermal transmittances in saturated state.

Sustrato	k_{dry} (W/m·K)	k_s(W/m·K)	R_s (m^2·K/W)	U_s (W/m^2·K)
S1	0.2500	0.7844	0.1912	5.2293
S2	0.1955	0.6132	0.2446	4.0883
S3	0.1000	0.3138	0.4781	2.0917

3.1.6. Permeability of geosynthetics

The permeability test perpendicular to a plane required time-consuming data processing, with the permeameter recording the variations in the height of the water column in the cylindrical pipes. This entailed a correction for viscosity, for which the temperature of the test water was recorded. The average velocity ($\overline{v_{h=50}}$) with which water permeates through the geotextile when the water column height over the tested specimen is 50 mm was found to be 43.4, 66.3 and 7.1 mm⁄s for geosynthetics G1, G2 and G3 respectively.

The geofoam (G3) clearly stands out from the other two geosynthetics due to its low permeability. It is understood that by opposing the passage of water, considerable water retention can be expected with respect to the other two materials, providing a greater amount of the available resource (cistern effect) for the plants rooted in the substrate placed on it.

As for the two more conventional geotextiles, the geocomposite (G1) showed a 35% lower permeability than the needled geotextile (G2). **Figure 8** shows the average curves as a function of the difference in water column height over the tested specimen, *h*. It can be seen that geosynthetics G1 and G2 display parabolic h-dependent permeability, reaching their maximum permeability at around 90 mm of water column height. The geofoam (G3), however, displays almost linear h-dependent permeability.

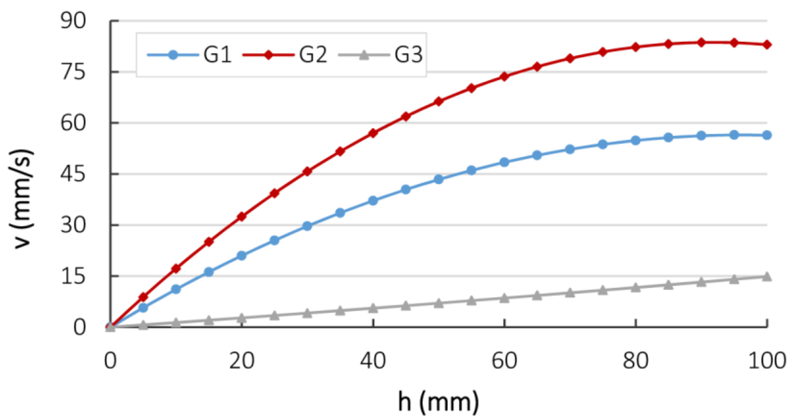

Figure 8. Average permeability curve in relation to water column height.

3.1.7. Permeability in composite sections

To evaluate the *Permeability* in the composite sections, it was necessary to relate it to the value of the equivalent precipitation, taking into account the recreated rainfall surface and the flows circulating through the irrigation system. The results obtained are shown in **Table 12**.

Table 12. *Permeability* test results in the composite section.

Substrate	Geotextile	Q $_{saturation}$ (l/h)	Equiv. rainfall (mm/h)	Permeability (mm/s)	Permeability Geotextile (mm/s)	Permeability Sust./Geotext. (%)
	G1	105	1167	0.32	43.4	0.74
S1	G2	120	1333	0.37	66.3	0.56
	G3	70	778	0.22	7.1	3.10
	G1	109	1211	0.34	43.4	0.78
S2	G2	113	1256	0.35	66.3	0.53
	G3	85	944	0.26	7.1	3.66
	G1	74	822	0.23	43.4	0.53
S3	G2	78	867	0.24	66.3	0.36
	G3	78	867	0.24	7.1	3.38

The decrease in permeability is univocally dependent on the substrates. This can be seen in the difference between the saturation flow rates of each of the samples tested and in the differences, within each type of substrate, among the geotextiles used. In the case of substrate S1, composed of universal substrate, limestone gravel and sand, the variability of permeabilities among the different geotextiles was remarkable in terms of equivalent rainfall admitted (from 778 mm/h with geofoam G3, to 1333 mm/h with needled geotextile G2, with a standard deviation of the equivalent rainfall of 285 mm/h), normalizing in terms of strict permeability (from 0.22 mm/s to 0.37 mm/s). This is indicative that the S1 mixture had a high permeability, admitting very heavy equivalent rainfall.

In the case of substrate S2, composed of universal substrate, crushed brick and sand, the variability of permeabilities was significantly lower, with equivalent rainfall ranging from 944 mm/h in the test with G3 geofoam to 1256 mm/h with G2 needled geotextile (standard deviation of the equivalent rainfall of 169 mm/h). Permeability stabilized around 0.32 mm/s, with a maximum of 0.35 mm/s for the G2 needle-punched geotextile and a minimum of 0.26 with G3 geofoam.

Finally, the S3 substrate in which the geofoam was added to S2 presented a permeability that could be considered homogeneous and equal to 0.24 mm/s. The standard deviation of the equivalent rainfall was reduced to 26 mm/h, so it could be considered homogeneous and of value 850 mm/h due to the precision of the manual measurement of the saturation flow rates and the limitations of the test system.

These values reflect a total dependence on the substrate, due to the perceptible differences between the results of each geotextile depending on the mixture with which they are combined. The permeability decreases significantly with respect to that of each geotextile, with the G3 geofoam undergoing the smallest decrease in percentage terms.

3.1.8. OM content of effluent water

Regarding the *Organic Matter (OM) Content* of the effluent water, it should be noted that all the sections tested complied with the potability criterion established by standard 2540 SOLIDS [71], according to which, water with values below 500 mg/l would be suitable. The results obtained are shown in **Figure 9**.

As can be seen, in general, the S1 substrate displayed greater variability, while the results were more homogeneous for the S3 substrate, at around 390 mg/l with hardly any variation between geotextiles. The latter suggests that the use of the S3 substrate achieved control of the organic matter contained in the effluent without notable dependence on the geosynthetic used.

Regarding the influence of the geotextiles, the effluent water of G1 has the lowest OM content for the three substrates, with its permeability and characteristic opening influencing the retention of organic matter as the water passes through. The opposite behaviour is generally observed in the case of G3, except in the combination with the S2 substrate, where the highest OM content corresponds to the G2 geotextile, which may be due to the lower fall of substrate through the joints of the geofoam blocks in the case of the G3 geotextile.

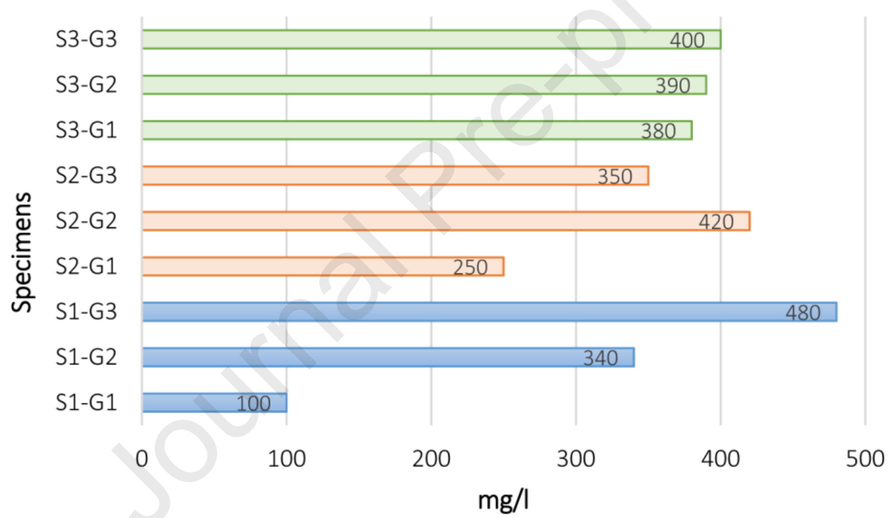

Figure 9. Organic matter content of the effluent.

3.1.9. Compaction of substrates

Based on the results of the bulk density test, the average compaction of each substrate after being subjected to the simulated rain was quantified. It should be noted that the thickness of the geotextile was not involved in any case, so this dimension did not affect the values provided. The results are shown quantitatively in **Table 13** providing the average heights (measured on each of the four sides of the test enclosure) of the substrate in each case, and relatively through the percentage of compaction observed.

Table 13. Compaction results.

Substrate	Geotextile	Reception height (cm)	Saturated height (cm)	Compaction (cm)
S1	G1	12.88	12.75	0.13 (0.97%)
	G2	12.50	12.40	0.10 (0.80%)
	G3	12.75	12.60	0.15 (1.18%)
S2	G1	12.65	12.58	0.07 (0.59%)
	G2	13.33	13.10	0.23 (1.69%)
	G3	13.83	13.78	0.05 (0.36%)
S3	G1	13.85	13.60	0.15 (1.81%)
	G2	14.38	13.88	0.50 (3.48%)
	G3	13.80	13.73	0.07 (0.54%)

Substrate S3 was by far the most compacted. The volume of the pieces and the fragility of the material are apparently the cause of this difference in volume. The S1 mix presented a slightly higher compaction than that observed in S2. The size of the gravel particles, larger than those of the crushed brick, caused the percentage of initial voids to be greater, reducing with the passage of water and causing a higher compaction.

In any case, the three measured compactions would not lead to a substantial difference that would compromise the integrity of the layer, its suitability for the vegetation cover or the drainage systems, if any. The change in volume should be taken into account, but in no case does it influence the correct function of the green roof.

3.1.10. Static puncturing of geosynthetics

As mentioned above, the static puncture resistance test was only performed on the G1 and G2 geosynthetics, recording the maximum force applied on the specimen until breakage, F_{max}, and the displacement associated with punch collapse, h_{max} (**Figure 10**). The results showed that the geocomposite (G1) withstood a 28% greater force, with a 20% lower maximum subsidence. This provides an idea of the greater stiffness provided by its woven polypropylene component, which gives the assembly greater strength by acting as reinforcement. On the other hand, the white geotextile (G2), being manufactured by means of a needle-punched structure, has a 'textile' structure that gives the material greater deformability, but lower maximum strength. In the application on green roofs, deformability would not be a requirement due to its direct placement on a rigid structure.

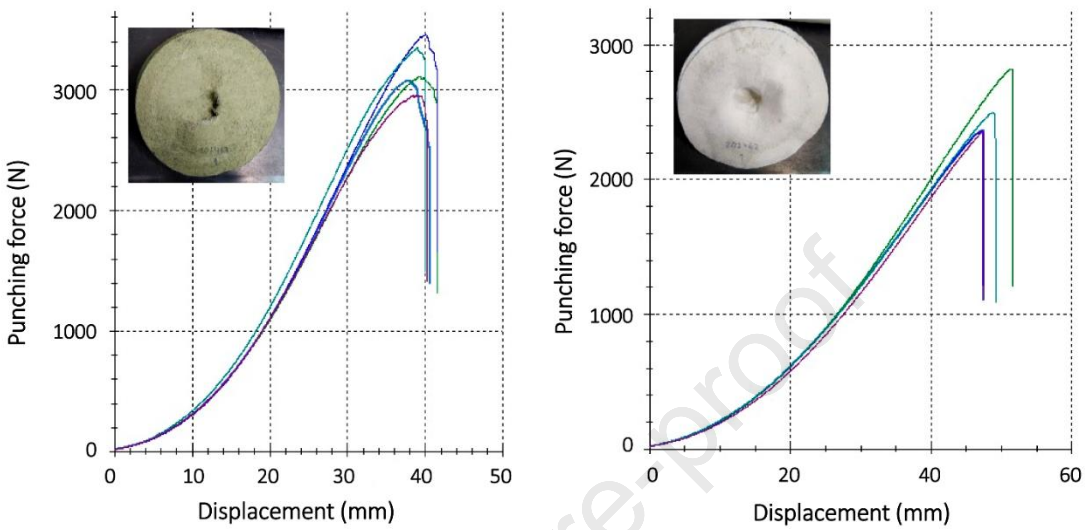

Figure 10. Static puncturing results G1 and G2, and appearance after tearing of the specimens.

3.1.11. Dynamic perforation of geosynthetics

The results obtained from the dynamic perforation test performed on the G1 and G2 geosynthetics yielded hole openings of 15.0 and 18.4 mm, respectively. Similarly to what was observed in the static puncture resistance test, the woven structure of the black and green geocomposite (G1) provides the material with a higher resistance, resulting in a smaller perforation than in the case of the white geotextile (G2). However, both perforations presented the same order of magnitude, which indicates that both geotextiles are designed for similar purposes or uses and give acceptable results in this test. It is considered that their response is sufficiently good and their performance on green roofs would be optimal. The appearance of both materials after the test is shown in **Figure 11**.

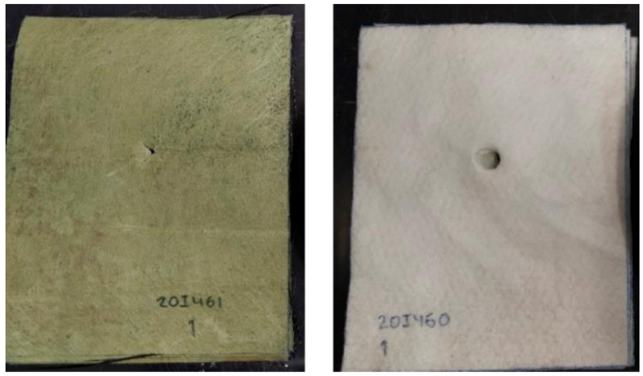

Figure 11. Appearance after dynamic perforation test of the G1 and G2 samples.

3.1.12. Characteristic opening of geosynthetics

The characteristic opening test is an indicator of the effective pore or void opening size of the tested material. The test results showed very different values. The geocomposite (G1) presented a characteristic opening significantly higher than the rest, 204 μm, a value that was almost three times that of the needled geotextile (G2), 76 μm. In any case, there was no risk of washout of fines, only the dissolution of part of the organic matter resulting from the passage of water. In the case of the geofoam (G3), a specific value could not be obtained due to the very small size of its pores. For its estimation, it was necessary to replace the filter piece of the solid material filtering cone with one of the same shape and size of geofoam. The test was carried out by pouring water together with the normalized black fine material of the test, obtaining as effluent clean water in which, if there were solid particles, these were not perceptible. After completion of the test, a maximum characteristic opening value of approximately 20 μm was established. **Figure 12** shows the test process and the appearance of the clear effluent water.

(a) (b)

Figure 12. (a) Characteristic opening test - Geofoam and (b) water passing through the geofoam with no appreciable presence of solids

3.1.13. Mass per unit surface area of geosynthetics

Regarding the analysis of the mass per unit area, its determination made sense only for geosynthetics G1 and G2. Since their third dimension (thickness) does not have a representative magnitude compared to the two dimensions that make up the surface of the geotextile, quantifying the mass per unit area is useful information when sizing covers and consulting industrial catalogues. However, in the case of geofoam (G3), its thickness becomes a sufficient entity to be considered. This differentiation becomes even more necessary after observing the variety of thicknesses of the geofoam pieces received in the laboratory, with thicknesses of approximately 1 cm to 2.5 cm (due to the cutting processes of the pieces when manufactured). Taking these aspects into account, **Table 14** shows the values obtained from the weighing and measurement of the specimens.

Table 14. Results of mass per unit area/volume.

Geosynthetic	**G1**	**G2**	**G3**
Mass/surface (g/m^2)	241	246	-
Mass/volume (kg/m^3)	-	-	22

From the results obtained, it can be seen that geosynthetics G1 and G2 have a very similar mass per unit area, which is positive since this will give greater relevance to the rest of the parameters when performing the multicriteria analysis. In this way, this indicator, which is not excessively relevant as established in the assignment of weights, will have even less impact on the conclusions of the analysis and will give prominence to more relevant parameters. On the other hand, geofoam (G3) showed a greater variability than the other two materials in the mass per unit volume measurements. This may be due to possible alterations suffered by the blocks during transport or handling, derived from the great fragility of the material.

3.1.14. Oxidation resistance of geosynthetics.

The oxidation test was carried out according to the corresponding standard, in this case UNE-EN ISO 13438:2020 [79]. The purpose was not to measure the variation of the physical-mechanical properties of the specimens but to measure the alteration of their hydraulic and filtering capacities. For this purpose, the specimens were kept in a hydrolysis tank for 2 days at 85 ºC and then subjected to a dry temperature of 105 ºC in an oven for 14 days. These conditions, according to UNE-EN ISO 13438, correspond to a deterioration period of 25 years.

In the case of geofoam (G3), significant surface oxidation was observed (**Figure 13**). The oxidation processes lead to an increase in the volume of the material, which leads us to assume in the first instance a decrease in the permeability of the material associated with the closure of the pore system. This was verified by means of a permeability test of the oxidized pieces in which, the non-validity of the expanded polystyrene (EPS) geofoam (G3) was confirmed for the corresponding normative test; it was not possible to balance the water columns in the two cylinders of the test apparatus, which leads to the conclusion that the material is not permeable. Cutting the material, it was verified that oxidation is not only superficial, but that it penetrates completely into the interior of the material.

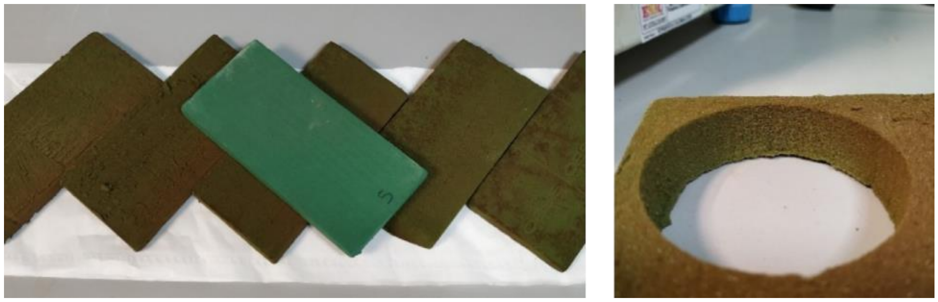

Figure 13. Results of the geofoam oxidation and alteration test.

The degradation process consisted of accelerating the oxidation of the geofoam by increasing the temperature (105 ºC), although without reaching the limit of softening of the material [85] in which the chains become agitated and form different connections, thus modifying the internal structure of the voids by deformation and so affecting, as has been proven, the permeability. Thus, it is evident that there is a risk of clogging not only due to physical clogging by fines entrained by the flow, but also due to oxidation of the material.

In addition, the characteristic opening size of the G1 and G2 geosynthetics was tested in order to quantify the variation of this property after 25 years of deterioration. The results obtained are shown in **Table 15**.

Table 15. Results of characteristic opening and permeability after oxidation resistance test.

Geosynthetic	**G1**	**G1-ox.**	**G2**	**G2-ox.**
Opening (µm)	204	147	76	87
	↓ 27.94 %		**↑ 14.47 %**	
$\bar{v}\ (mm/s)$	43.4	32.0	66.3	61.6
	↓ 26.27 %		**↓ 7.09 %**	

The G1 geocomposite underwent a considerable decrease of almost 28% of its characteristic opening, while the G2 geosynthetic underwent an increase of lesser magnitude. It could be considered that the result of alteration of this property is not conclusive since the response is not homogeneous, although the chemical composition of the geosynthetics is the same. However, relationships could not be established as a larger number of tests would be necessary to establish these. One of the reasons for this difference may be the irregularity of G1 and specially G2, since, in their state of reception, and due to the physical characteristics of the products, they present areas with slight 'bald spots'.

Geosynthetics G1 and G2 were also tested for permeability, comparing their hydraulic behaviour with the behaviour under reception conditions (**Figure 14**). A decrease in permeability was observed in both materials, this being more significant in the G1 geocomposite with a decrease of 26.27%, while the needled geotextile (G2) underwent a more moderate decrease of 7.09%, the deterioration being homogeneous in all the tested specimens, **Table 15**. **Figure 15** illustrates the results obtained. It can be seen that for the geocomposite (G1), the permeability decreased at lower values of h, clearly and evidently departing from the permeability curve in the as-received state. In the case of the needled geotextile (G2), the maximum differences were observed between 40 and 60 mm, presenting magnitudes close to those of the curve in the as-received condition for extreme h values. This shows that both materials have an acceptable behaviour against oxidative processes, the resistance of the white polypropylene geotextile (G2) being notably superior, undergoing very reduced variations in permeability.

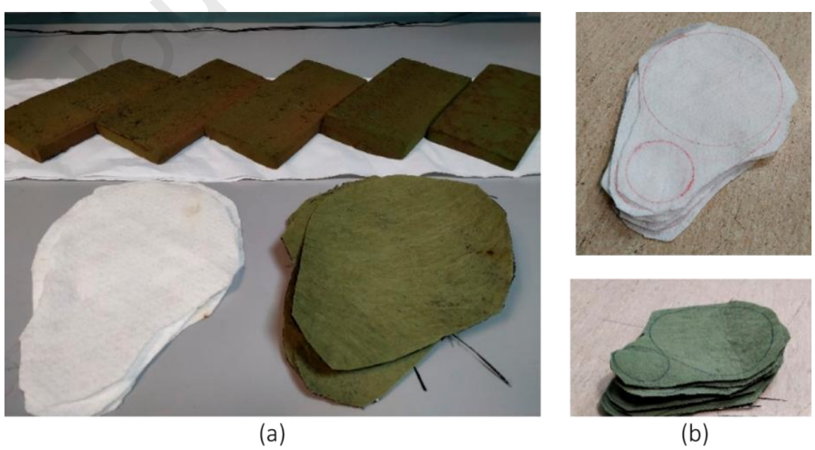

Figure 14. (a) Specimens extracted from the furnace - Oxidation and (b) samples in the as-received state.

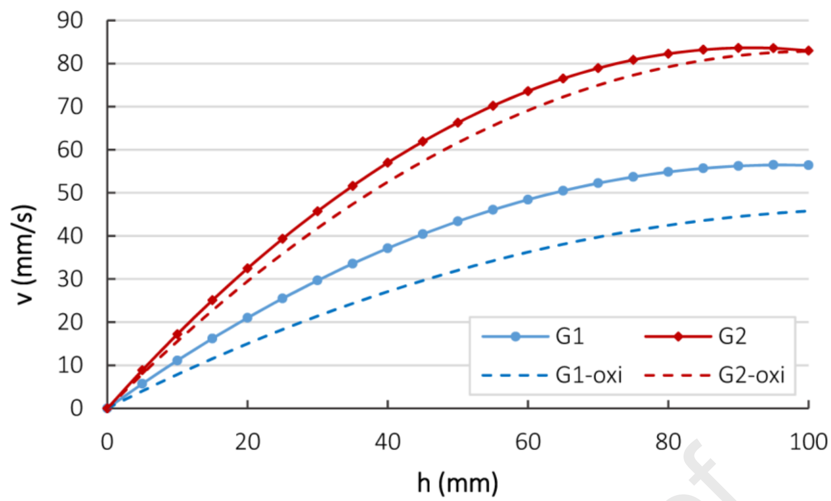

Figure 15. Oxidation results. Evolution of permeability with respect to different water column heights (h).

Finally, the geofoam (G3) underwent an appreciable colour change. This alteration was measured by colorimetry using the CIEDE2000 method [86]. In this standard, a three-dimensional colour space is generated to represent the values (X, Y, Z) on normalized rectangular coordinates as non-linear functions. The numerical values represent relative colour differences in Euclidean and vector form. The three axes relate to the chromatic spectra black/white (L), green/red (a) and blue/yellow (b). The results obtained are shown in **Table 16**, where L, a, b are relative units within the colour coordinate system of the method used, ΔL, Δa, Δb are the variations of these units, and ΔE_{oo} is the variation vector resulting from colorimetry. The changes obtained were evident, with the colour darkening slightly and taking on a noticeably browner tone. Take into account that a ΔE_{oo} higher than 3 implies a colour difference detectable by the mean human eye. These are shades that are clearly associated with oxidation, the magnitude of the changes demonstrating the strong sensitivity of the geofoam to this process.

In view of the tests carried out, it can be stated that oxidation affects G3 considerably and G1 to a lesser extent, but it would be necessary to develop a more in-depth study to conclude with greater precision the effect on the G2 geocomposite.

3.1.15. Hydrolysis resistance of geosynthetics.

The hydrolysis test was carried out according to the conditions established by UNE-EN ISO 12447 [78], but with the objective of evaluating the materials not under tensile stress, as required by the latter, but against permeability and characteristic opening, thus verifying the alterations suffered in their hydraulic and filter properties. After 4 days subjected to 95 ºC, a large effect of this process could be appreciated on the geofoam (G3), which underwent an evident change of colour in this short period, corresponding to 6.67 years according to the equivalence established by the UNE-EN ISO 12447. This alteration was measured through colorimetry, applying the CIEDE2000 method [86]. Three readings were taken of the material subjected to hydrolysis, comparing them with the standard measured on a piece in the as-received state. The results obtained are shown in **Table 16** and **Figure 16**.

Table 16. Colorimetry results after hydrolysis and oxidation resistance tests.

Measure	Oxidation				Hydrolysis			
	G3-1	G3-2	G3-3	Media	G3-1	G3-2	G3-3	Media
L	33.22	32.20	33.16	32.86	38.07	38.41	38.26	38.25
a	1.42	6.77	2.94	3.71	-11.66	-11.70	-11.27	-11.54
b	20.70	20.81	20.79	20.77	14.56	14.42	14.40	14.46
ΔL	-6.63	-7.65	-6.69	-6.99	-1.78	-1.44	-1.59	-1.60
Δa	16.78	22.12	18.30	19.07	3.70	3.66	4.08	3.81
Δb	12.41	12.52	12.50	12.48	6.28	6.14	6.11	6.18
ΔE_{00}	19.50	24.81	20.97	21.76	5.71	5.55	5.81	5.69

(a) (b)

Figure 16. (a) Colorimetry test performed on G3 samples after hydrolysis test, and (b) difference in appearance between sample on reception (left) and after hydrolysis (right).

In addition, and due to the considerable reduction in permeability observed in the geocomposite (G1) in the oxidation test, the possible alteration of this property during the hydrolysis process was studied. Thus, despite corresponding to a simulated period of less than 7 years as mentioned above, the reduction in permeability, **Table 17**, is very similar to that undergone due to oxidation, suggesting that the geocomposite (G1) is equally sensitive to hydrolysis processes.

Table 17. Permeability results after hydrolysis resistance test.

Geosynthetic	G1	G1-hybrid
$\bar{v}\,(mm/s)$	43.4	31.4
	↓ 27.65 %	

3.2. ELECTRE method results

Once the indicators had been analysed, it was necessary to carry out a qualitative analysis that contrasted the performance of the materials tested with respect to what was expected of them (based on the usual values of contrasted green roof products) and compared them among themselves. For this assessment, the main objective of the study, sustainability, was not ignored, so that not only were weights assigned to each indicator, but the suitability of the properties of each material and/or composite section was also studied.

The evaluation was carried out independently for each indicator, so that through the evaluation matrix the results were combined to extract a common conclusion for each of the three groups considered: substrate, geotextile and composite section (substrate + geotextile). In this way, the ideal material for each application was evaluated independently along with the best combination, extracting the ideal composite section for the criteria contemplated in this research.

3.2.1. Substrate

Taking into account the weights assigned to the indicators corresponding to the evaluation of the substrates, the values obtained from the calculations and the tests carried out, and applying the principles of sustainability, the different alternatives considered (S1, S2 and S3) were rated, **Table 18**.

Table 18. Qualification of substrate alternatives.

Indicator	Weight	S1	S2	S3
Life cycle cost	4	5	5	3
Carbon footprint	2	4	5	3
OM Composition	1	3	2	5
Thermal insulation (U)	3	2	3	5

The criteria applied to assign the respective ratings were as follows:

- **Life cycle cost**: the highest score (5) was assigned to substrates S1 and S2 which had the lowest life cycle cost according to the estimates made. As for S3, it obtained a score of 3 points in proportion to the higher value of the indicator with respect to the other two alternatives mentioned (37.53% higher).
- **Carbon footprint:** the highest score (5) was awarded to the substrate with the lowest impact (S2), decreasing by one point for each consecutive substrate in increasing order of impact on the carbon footprint.
- **Composition in OM**: the substrate with the highest organic matter content (S3) was assigned the highest score (5). The following mixtures, in decreasing order, were assigned ratings of 3 and 2 respectively, none of them being rated 4 due to the substantial difference compared to S3.
- **Thermal insulation (U)**: the highest grade (5) was assigned to substrate S3, which had the lowest thermal transmittance and, therefore, the highest insulation. Following this reasoning, grades of (2) and (3) were established for substrates S1 and S2 respectively due to the higher magnitude of their transmittances.

After this approach, the concordance and discordance matrices were calculated. Finally, the probable and real dominances were calculated (only in the case of probable dominance was it verified whether there was real dominance, verifying the superiority of one alternative over the other), **Table 19**.

Table 19. Substrate dominance.

Probable dominance	Real dominance
If CSi/Sj ≥ P, Si is likely to dominate Sj	***If DSi/Sj ≤ Q, Si is likely to dominate Sj***
9>5.67 → S2 probably dominates S1	*1 < 1.83* → S2 really dominates S1
6 > 5.67 → S1 probably dominates S3 *6 > 5.67* → S2 probably dominates S3	*There are no real dominances*
Probable dominance	***Real dominance***
If CSi/Sj < P, Si is likely to be dominated by Sj	***If DSi/Sj > Q, Si is likely to be dominated by Sj***
5 < 5.67 → S1 is probably dominated by S2	*There is no real dominance*
4 < 5.67 → S3 is probably dominated by S1 *4 < 5.67* → S3 is probably dominated by S2	*3 > 1.83*→ S3 is really dominated by S1 *2 > 1.83*→ S3 is really dominated by S2

The reading given by the substrate dominance table is not entirely decisive. On the one hand, the concordance matrix shows that there is real dominance of S2 over S1, without concluding any real dominance over S3. However, through the discordance matrix, the dominance of S2 over S1 is denied, but the dominance of these two over S3 is confirmed. From this, it can be concluded that both substrate mixtures are sufficiently valid at a similar level, within the selected indicators, each of them being more suitable for specific climatic conditions and vegetation cover, depending on the desired use of the cover and its location. Moreover, in view of the results obtained, given that a real dominance of S2 over S1 has been shown (although the discordance analysis has not confirmed that S1 is really dominated by S2), the following order of choice could be proposed as a result of the study: **(S2 > S1) >> S3**. In this case, the recycled material component played a decisive role in favour of S2 as it contained crushed brick. However, despite its high insulation performance, S3 has been significantly penalized by its economic and environmental impact through life cycle cost and carbon footprint indicators.

3.2.2. Filtering separating layer (geotextile)

The different alternatives contemplated for the geotextiles (G1, G2 and G3) were similarly rated, **Table 20**.

Table 20. Qualification of geotextile alternatives.

Indicator	Weight	G1	G2	G3
Permeability	9	4	5	2
Life cycle cost	8	5	5	2
Carbon footprint	3	3	4	5
Static puncturing	6	5	4	1
Dynamic perforation	7	5	4	1
Characteristic opening	2	3	4	5
Mass per unit of surface area	1	4	4	4
Hydrolysis resistance	4	3	4	1
Oxidation resistance	5	3	5	1

In this case, the criteria applied to assign the respective ratings were as follows:

- **Permeability**: given the importance of green roofs to buffer rainfall events, especially those of great magnitude, their components are required to have high permeability, thus preventing water accumulating, increasing the weight of the system and generating conditions that are not suitable for plant development. Because of this, the highest score (5) was awarded to the geotextile (G2), which presented the highest permeability. The geofoam was rated with a lower score (2), due to the difference in magnitude of this property with respect to the other materials.
- **Life cycle cost**: the highest score (5) was assigned to geotextiles G1 and G2, which had the lowest life cycle cost according to the estimates made. As for G3, it obtained a score of (2) points in proportion to the value of the indicator with respect to the other two alternatives mentioned (42.78% higher).
- **Carbon footprint**: the highest rating was assigned to the geotextile (G3) that caused the least impact in carbon equivalent emissions, with the rating decreasing as this impact increases.

- **Static puncture resistance:** in this case, geotextiles G1 and G2 showed very similar results, although G1 performed somewhat better. On the other hand, G3 is penalized due to its poor static puncture resistance.
- **Dynamic perforation**: the reasoning followed for this indicator was the same as that followed for the preceding indicator.
- **Characteristic opening:** the criterion followed to award the scores for this indicator is related to the filtering capacity. Thus, geofoam (G3) achieved the highest score as it had the smallest characteristic opening, since it retained a greater amount of fines than the other materials. Consequently, the ratings given to the other two materials were lower as their characteristic aperture was higher.
- **Mass per unit surface area**: the three geotextiles were assigned a rating of (4) as they had values of mass per unit area (unit volume in the case of G3) of a similar magnitude, and because of their low variation with respect to the effects they could have on a vegetated canopy.
- **Hydrolysis resistance:** an intermediate grade (3) was awarded to G1, in view of the considerable reduction in its permeability. The geofoam (G3) underwent evident alterations, so the rating awarded to it was the lowest. On the other hand, G2 was assigned a value (4), not awarding it the maximum value because, after the tests carried out, it cannot be stated that the effect is null or almost null.
- **Oxidation resistance**: in this case, the effect on G1 was not entirely clear; a more in-depth study would be necessary to draw more categorical conclusions, so it was given an intermediate grade (3) in view of the worsening of its properties. In the case of the G2, the effect was scarce, so it was given the highest grade (5), and the lowest grade was assigned to the geofoam (G3), given the very poor results achieved.

Then, after calculating the concordance and discordance matrices, the probable and actual dominances obtained are shown in **Table 21**. This suggests that there is a considerable dominance of the G2 geosynthetic over G1, without guaranteeing the dominance of any of them over the geofoam (G3). However, the low performance of the latter is evident in the concordance matrix as it clearly provides insufficient resistance to several of the tests contemplated, not guaranteeing correct operation of the system without suitable maintenance and, in any case, it is notably costlier.

In parallel to what was observed with the substrate mixtures analysed, the second option seems to outperform the other two, among other reasons thanks to its partly recycled or reused composition and the relevance of the indicators that are linked to this aspect. Thus, it can be concluded that for a generic case, the order of dominance of the geotextiles studied is **(G2 >> G1)** > **G3**, the white needle-punched geotextile being clearly better in applications as a separating layer on green roofs.

Table 21. Geotextile dominances.

Probable dominance	**Real dominance**
If CSi/Sj ≥ P, Si is likely to dominate Sj	***If DSi/Sj ≤ Q, Si is likely to dominate Sj***
40>24.33 → G1 probably dominates G3 *40>24.33* → G2 probably dominates G3	*There are no real dominances*
39 > 24.33 → G2 probably dominates G1	*2< 2.33* → G2 really dominates G1
Probable dominance	***Real dominance***
If CSi/Sj < P, Si is likely to be dominated by Sj	***If DSi/Sj > Q, Si is likely to be dominated by Sj***
15 < 24.33 → G1 is likely to be dominated by G2	*There is no real dominance*
6 < 24.33 → G3 is likely to be dominated by G1 *6 < 24.33* → G3 is likely to be dominated by G2	*There are no real dominances*

3.2.3. Composite section (substrate-geotextile)

In line with what was proposed for the substrate and the geotextile, the composite section was analysed. Considering the values obtained from the calculations and tests carried out, and applying the principles of sustainability, the 9 different alternatives contemplated for the composite sections were rated as follows (Si-Gj), **Table 22**.

Table 22. Qualification of composite section alternatives.

Indicator	Weight	S1G1	S1G2	S1G3	S2G1	S2G2	S2G3	S3G1	S3G2	S3G3
Bulk density	3	2	2	2	3	3	3	5	5	5
Saturated density	4	2	3	3	3	3	3	3	3	4
Permeability	5	4	5	2	5	5	3	3	3	3
Effluent OM content	1	5	3	2	4	2	3	3	3	2
Compaction	2	4	4	3	4	2	5	2	1	4

The criteria applied to assign the respective ratings in this case were as follows:

- **Bulk density**: the highest rating was assigned to the sections in which the S3 substrate is placed as they have by far the lowest dry density. Those in which the S1 and S2 substrates are located were given lower ratings based on their higher measured density.
- **Saturated bulk density**: as in the previous indicator, the highest score was awarded to the section with the lowest density. In this case the densities are quite similar, so S3G3 was assigned (4), not receiving the maximum value as it underwent a considerable increase from the as-received state; S1G1 (2) as it had the highest saturated density, and (3) for the rest of the sections tested.
- **Permeability**: those substrate-geotextile pairs with permeability greater than 1200 mm/h of equivalent rainfall received the maximum rating (5). Between 1000 mm/h and 1200 mm/h a rating of (4) was assigned. Those with equivalent rainfall between 800-1000 mm/h were given (3). Finally, the composite section with permeability less than 800 mm/h (S1G3) was assigned (2). It should be mentioned that, as explained above, the performances of all the combinations tested are good and meet the requirements demanded of a green roof. The differentiation in terms of rating assigned to them is due to the need to highlight the different orders of magnitude, given the great importance of the indicator in question.
- **Effluent OM content**: in this case, since all the results comply with the 500 mg/l limit, all the effluent waters would be considered potable when only this indicator was taken into account. However, and given that the intention is to compare alternatives and not to comply

with standards (in the same way as occurs with permeability), it was considered appropriate to assign scores that would highlight the differences with respect to this parameter. For this reason, it was decided to give (5) to those samples with an effluent OM content between 100-200 mg/l, (4) for those with values between 200-300 mg/l, (3) for values between 300-400 mg/l and (2) to those with a content between 400 mg/l and the 500 mg/l limit.

- **Compaction**: the sections tested presented reduced compaction values, but it was decided to differentiate the results through the scores, so that (5) was assigned to compaction between 0-0.5%, (4) to that between 0.5-1.0%, (3) to that between 1.0-1.5%, (2) up to 2.0% and (1) to that higher than 2.0%.

Then, after the corresponding calculation of the concordance and discordance matrices, the probable and real dominances were calculated (only in the case of probable dominance is it verified whether there is real dominance, certifying the superiority of one alternative over the other), the results of which are shown in **Table 23**.

Table 23. Composite section dominances.

Probable dominance	**Real dominance**
If CSi/Sj ≥ P, Si is likely to dominate Sj	***If DSi/Sj ≤ Q, Si is likely to dominate Sj***
15 > 9.93 → S1G2 probably dominates S1G3	*No real dominance of S1G2 over S1G3*
15 > 9.93 → S2G1 probably dominates S1G2, S1G3 and S2G2	*1 < 1.875* → S2G1 really dominates S1G2, but there is no real dominance over S2G2 and S2G3
15 > 9.93 → S2G3 probably dominates S1G3	*1 < 1.875* → S2G3 really dominates S1G3
15 > 9.93 → S3G1 probably dominates S3G2	*1 < 1.875* → S3G1 really dominates S3G2
15 > 9.93 → S3G3 probably dominates S1G3	There is no real dominance of S3G3 over S1G3
14 > 9.93 → S1G2 probably dominates S1G1	*1 < 1.875* → S1G2 really dominates S1G1
14 > 9.93 → S2G1 probably dominates S1G1	*1 < 1.875* → S2G1 really dominates S1G1
14 > 9.93 → S3G3 probably dominates S3G1 and S3G2	*There is no real dominance*
13 > 9.93 → S2G1 probably dominates S2G3	*There is no real dominance*
13 > 9.93 → S2G2 probably dominates S1G3	*There is no real dominance*
13 > 9.93 → S3G1 probably dominates S1G3 and S2G3	*There are no real dominances*
13 > 9.93 → S3G2 probably dominates S1G3, S2G3 and	*0 < 1.875* → S3G2 really dominates S3G1, but there is

S3G1	no real dominance over S1G3 or S2G3
12 > 9.93 → S1G2 probably dominates S2G2, S3G1 and S3G2	*1 < 1.875* → S1G2 really dominates S2G2, but there is no real dominance over S3G1 and S3G2
12 > 9.93 → S2G1 probably dominates S3G1 and S3G2	There are no real dominances
12 > 9.93 → S2G2 probably dominates S1G1, S1G2, S2G1 and S2G3	*1and 0 < 1.875* → S2G2 really dominates S1G1, S1G2 and S2G1, but not S2G3
12 > 9.93 → S2G3 probably dominates S3G1 and S3G2	*There are no real dominances*
12 > 9.93 → S3G3 probably dominates S2G3	*There are no real dominances*
11 > 9.93 → S1G1 probably dominates S1G3	*There is no real dominance*
11 > 9.93 → S2G2 probably dominates S3G1 and S3G2	*There are no real dominances*
10 > 9.93 → S1G2 probably dominates S2G3	*There is no real dominance*
10 > 9.93 → S2G3 probably dominates S1G2 and S2G2	*1 < 1.875* → S2G3 really dominates S1G2, but there is no real dominance over S2G2
10 > 9.93 → S3G1 probably dominates S2G2	
10 > 9.93 → S3G3 probably dominates S2G2	*There are no real dominances*
Probable dominance	***Real dominance***
If CSi/Sj < P, Si is likely to be dominated by Sj	***If DSi/Sj > Q, Si is likely to be dominated by Sj***
9 < 9.93 → S2G3 is likely to be dominated by S1G1 and S2G1	*There are no real dominances*
9 < 9.93 → S3G1 is likely to be dominated by S3G3	*There is no real dominance*
9 < 9.93 → S3G2 is likely to be dominated by S3G3	*There is no real dominance*
9 < 9.93 → S3G3 is likely to be dominated by S1G1, S1G2 and S2G1	*3 and 2 > 1.875* → S1G1, S1G2 and S2G1 really dominate S3G3
8 < 9.93 → S1G1 is likely to be dominated by S3Gj	*3 and 2 > 1.875* → S3Gj really dominates S1G1
8 < 9.93 → S1G2 is likely to be dominated by S3G3	*2 > 1.875* → S3G3 really dominates S1G2
8 < 9.93 → S2G1 likely to be dominated by S3G3	*2 > 1.875* → S3G3 really dominates S2G1
8 < 9.93 → S2G3 is likely to be dominated by S3G3	There is no real dominance
8 < 9.93 → S3G1 is likely to be dominated by S1G2	*3 > 1.875* → S1G2 really dominates S3G1
8 < 9.93 → S3G2 is likely to be dominated by S1G2 and S2G2	*3 and 2 > 1.875* → S1G2 and S2G2 really dominate S3G2
7 < 9.93 → S1G2 is likely to be dominated by S2G1	There is no real dominance
7 < 9.93 → S1G3 is likely to be dominated by S1G1, S1G2 and S2G2	There are no real dominances
7 < 9.93 → S3G1 is likely to be dominated by S1G1 and S2G1	*3 and 2 > 1.875* → S1G1 and S2G1 really dominate S3G1
7 < 9.93 → S3G2 is likely to be dominated by S1G1 and S2G1	*3 and 2 > 1.875* → S1G1 and S2G1 really dominate S3G2
6 < 9.93 → S1G1 is likely to be dominated by S1G2 and	*2 > 1.875* → S1G2 and S2G3 really dominate S1G1

S2G3 *6 < 9.93* → S1G3 is likely to be dominated by S3G1 and S3G2 *6 < 9.93* → S2G2 is likely to be dominated by S3G3	*2 > 1.875* → S3G2 really dominates S1G3, but S3G1 does not *2 > 1.875* → S3G3 really dominates S2G2
4 < 9.93 → S1G3 is likely to be dominated by S2G1 and S2G3	There are no real dominances
3 < 9.93 → S1G1 is likely to be dominated by S2G1 and S2G2	*3 > 1.875* → S2G2 really dominates S1G1, but S2G1 does not
1 < 9.93 → S1G3 is likely to be dominated by S3G3	There is no real dominance

The actual dominances resulting from the analysis were inconclusive, showing some degree of contradiction regarding the dominance of some pairs of composite sections. Generally speaking, the sections in which the third type of substrate (S3Gj) was used seem to be dominated by the rest, with the exception of section S3G3, which was apparently superior to others. This superiority is not explained by the results obtained for geofoam as a separating layer (G3), or as a material included in the substrate mix (S3), cases in which its poorer performance was demonstrated according to the criteria defined by this project.

As a result of the dominance table, and in spite of the contradictions existing, an order of suitability of the composite sections is proposed as a first approximation: S3G3 > (S2G1, S2G2, S2G3) > S1G2 > (S3G1, S3G2, S1G1) > S1G3. However, the following comments should be made:

- Fundamentally in terms of material densities, both in the as-received state (bulk density) and in saturation, the S3 substrate made the difference, giving the composite sections containing it an advantage over the others thanks to its lightness.
- Regarding permeability, the most relevant indicator as established in this research, its performance was good as it complies with the standards required for installation in a vegetative roof, but as it is poorer than the rest, it receives a notable penalty.
- Within the composite sections containing S3, there is no real dominance; therefore, based on this analysis, it would not be possible to establish an order of priority among them. However, based on

the conclusions drawn from the detailed analysis of the separating layer, it seems logical to state that S3G2 > S3G1 > S3G3. Establishing this order among the S3Gj sections, the S3G3 section would be rejected.

- Similarly, as was justified when discussing the three substrate solutions, the superiority of S2Gj, sections in which recycled material is available within the substrate mix, should be highlighted. In general, these composite sections achieved the best permeability performance and provided reasonable performance in terms of densities (apparent and saturated), effluent OM content and compaction, with section S2G1 outperforming the others.
- With regard to S1Gj sections, their overall performance is lower than S2Gj and higher than S3Gj sections, with the exception of the S1G3 section, whose performance was the worst of the options considered, according to the criteria established.

Therefore, considering all the tests carried out and based on the comments above, the following order of suitability is finally proposed: **(S2G1 > S2G2)** >> **S1G2** >> **S2G3** >> **S1G1** >> **(S3G2 > S3G1 > S3G3)** >> **S1G3**.

It is necessary to clarify that, given the unsuitability of geofoam as a separating layer (G3), its use was not considered suitable in this application for green roofs, which is not reflected in this order of suitability of composite sections because the properties that cause it to be discarded correspond to the detailed analysis of geotextiles and not to that of the total section.

In summary, in view of the results of the analysis carried out on the composite sections and the detailed analysis for substrates and separating layers, it can be concluded that, in order to improve the resilience of cities and to make constructions as sustainable as possible, it is necessary to use recycled or reused materials that favour adequate hydraulic behaviour of the roof, as long as they present properties that meet the minimum requirements demanded of any material used in roof construction.

4. Conclusions

Green roofs are a solution to increase the sustainability of buildings due to their multiple benefits in terms of social, economic, and environmental advantages. Despite the great amount of research on green roofs in the literature, it is not so easy to find experimental studies that analyse the suitability of the green roof layers. Therefore, this study assessed the effect of nine different combinations of substrate-geotextile (filter membrane) in green roofs. The methodology defined involves a comparison between a common material frequently used in green roof applications, a recycled or reused material, and a proposal for novel materials. When studying the substrate and geotextile layers, it became necessary to define a series of indicators that could be measured during the experimental campaign.

The ELECTRE method was selected as a multi-criteria analysis method. It is widely used in studies of this type, so its application in this case seems appropriate. However, it has demonstrated certain limitations in indicating the most appropriate option among the composite sections studied, not specifying the dominance between some pairs, which has meant the application of common sense was necessary to establish a definitive order.

It can be stated that the sustainability objectives required for these upper layers of a green roof have been achieved, resulting in sufficiently valid typologies. In general, the substrate mixtures considered have provided adequate performance complying with the expected standards.

The values for life cycle cost and carbon footprint demonstrate the benefits of using recycled materials, especially when they come from the construction sector itself, thus facilitating the creation and consolidation of synergies in the use of materials and processes. For example, in terms of carbon footprint, substrate S2, made of crushed brick, silica sand and compost, presents a Global Warming Potential of 3.51 kg CO_2 eq. 100 years, which supposes a reduction of 19.86% in relation of S1 and 26.72% in relation of S3. There is a clear need to increase the ratio of recycled or reused materials used in new constructions, thus reducing emissions generated per unit of built surface and reducing as much as possible the amount of waste generated in a high impact sector such as construction.

Regarding the geotextiles used as a separating layer, it is important to point out the unsuitability of geofoam (G3) for this application. In spite of having provided good results in its incorporation into the substrate layer, in the case of the separating layer, its properties, especially the hydraulic and physical ones, as well as its resistance to deterioration processes (hydrolysis and oxidation), do not reach the minimum standard required to be considered a suitable material. The fact that it does not guarantee correct hydraulic operation makes it a material to be discarded, since it would compromise the operation of the system by penalizing the most important indicator among those considered (permeability). The permeability ($\overline{v_{h=50}}$) of geotextile G3 is 7.1 mm⁄s, which represents 16.36% and 10.71% in relation to permeability of G1 and G2, respectively. The other two materials studied, green-black geocomposite (G1) and white needle-punched geotextile (G2), performed acceptably; they responded adequately to environmental deterioration processes (especially G2), in addition to having shown sufficient resistance to the stresses inherent to site work such as static puncturing and dynamic perforation. In this way, the woven structure of the geocomposite G1 provides the material with the highest resistance, which withstood a 28% greater force than G2 in the static puncturing test, and a smaller hole opening in the dynamic perforation test (15.0 and 18.4 mm in G1 and G2, respectively). When selecting one of these two geotextiles, it would be preferable to choose the reused geotextile (G2), given its better hydraulic performance and, especially, since this does not penalize its properties. However, it would be interesting to study other reused geotextiles with potential application in vegetative roofs and contrast the results with respect to totally new material. In this way, its suitability for this use could be validated since, in case of demonstrating a suitable performance for this application, the spectrum of potentially valid geocomposites for use as a separating layer in green roofs would be expanded.

Regarding the black-green geocomposite (G1), in view of the results obtained in the hydrolysis and oxidation resistance tests, with decrease in permeability of 27.65% and 26.27% respectively in relation of the values measured previously to the deterioration processes, it seems necessary to extend its study by testing a larger number of specimens to analyse the variability observed in its properties.

Regarding the composite sections studied, the ones with substrate S2, which include reused or recycled material, generally show higher performance than the rest of the sections studied. Thus, section S2G1 followed by S2G2 provided the best results and responded most adequately to the proposed indicators and criteria. Their high permeability (0.34 and 0.35 mm/s, respectively), low organic matter content of the effluent (250 and 420 mg/l, both values are suitable according to the standard 2540 SOLIDS) and adequate density (1031.53 and 1030.56 kg/m^3) make them highly attractive sections to be incorporated into a green roof. The hydraulic properties of this pair of materials (substrate-geotextile) guarantee an optimum rainfall buffering, being suitable for very rainy climates or those in which rainfall phenomena are short, but of considerable intensity.

It is worth mentioning that all the sections tested demonstrated correct hydraulic performance, withstanding equivalent rainfall and guaranteeing a good response to peak rainfall events. These sections guarantee the conservation of the structure of the substrate-geotextile system, maintaining its thickness practically constant (with compaction ranging from 0.36% to 3.48%) and without loss of fines that would diminish the properties of the substrate and, therefore, could compromise in the medium or long term the availability of nutrients to the vegetation cover.

Likewise, it should be noted that, with any of the sections contemplated, the quality of the effluent water would be adequate for human consumption in terms of organic matter content, requiring the analysis of other compounds so that this consumption is guaranteed. However, organic matter would also serve as an indicator of the fine particle retention capacity of the separating layer.

Acknowledgements

This research was supported by the project "Caracterización mecánica de secciones filtrantes y estrategias de localización inteligente para un drenaje urbano sostenible a escala ciudad" (RTI2018-094217-B-C32, MCIU/AEI/FEDER, UE) of the 2018 Call for R+D+i projects «Retos investigación» of the "Programa Estatal de I+D+i Orientada a los retos de la Sociedad".

References

[1] B. Bhatta, Causes and Consequences of Urban Growth and Sprawl. In: Analysis of Urban Growth and Sprawl from Remote Sensing Data. Advances in Geographic Information Science. Springer, Berlin, Heidelberg, 2010. https://doi.org/10.1007/978-3-642-05299-6_2.

[2] M. Lin, J. Dong, L. Jones, J. Liu, T. Lin, J. Zuo, H. Ye, G. Zhang, T. Zhou, Modeling green roofs' cooling effect in high-density urban areas based on law of diminishing marginal utility of the cooling efficiency: A case study of Xiamen Island, China, J. Clean Prod. 316 (2021) 128277. https://doi.org/10.1016/j.jclepro.2021.128277.

[3] E. Cuce, Thermal regulation impact of green walls: An experimental and numerical investigation, Appl. Energy 194 (2017) 247-254, https://doi.org/10.1016/j.apenergy.2016.09.079.

[4] M. Santamouris, Cooling the cities - A review of reflective and green roof mitigation technologies to fight heat island and improve comfort in urban environments, Sol. Energy 103 (2014) 682-703, https://doi.org/10.1016/j.solener.2012.07.003.

[5] H. Frumkin, Urban sprawl and public health, Public Health Rep. 117 (3) (2002) 201-217, http://dx.doi.org/10.1016/S0033-3549(04)50155-3.

[6] S.S. Herrera-Gomez, A. Quevedo-Nolasco, L. Pérez-Urrestarazu, The role of green roofs in climate change mitigation. A case study in Seville (Spain), Build. Environ. 123 (2017) 575-584, https://doi.org/10.1016/j.buildenv.2017.07.036.

[7] B. Stone, Urban sprawl and air quality in large US cities, J. Environ. Manage. 86 (4) (2008) 688-698, https://doi.org/10.1016/j.jenvman.2006.12.034.

[8] E. Cuce, S.B. Riffat, A smart building material for low/zero carbon applications: heat insulation solar glass-characteristic results from laboratory and in situ tests, Int. J. Low-Carbon Technol. 12 (2) (2016) 126-135, https://doi.org/10.1093/ijlct/ctw009.

[9] A.B. Besir, E. Cuce, Green roofs and facades: A comprehensive review, Renew. Sust. Energ. Rev. 82 (Part 1) (2018) 915-939, https://doi.org/10.1016/j.rser.2017.09.106.

[10] A.M. Coutts, E. Daly, J. Beringer, N.J. Tapper, Assessing practical measures to reduce urban heat: Green and cool roofs, Build. Environ. 70 (2013) 266-276, https://doi.org/10.1016/j.buildenv.2013.08.021.

[11] P. Bevilacqua, The effectiveness of green roofs in reducing building energy consumptions across different climates. A summary of literature results, Renew. Sust. Energ. Rev. 151 (2021) 111523, https://doi.org/10.1016/j.rser.2021.111523.

[12] R. Berto, C.A. Stival, P. Rosato, Enhancing the environmental performance of industrial settlements: An economic evaluation of extensive green roof competitiveness, Build. Environ. 127 (2018) 58-68, http://dx.doi.org/10.1016/j.buildenv.2017.10.032.

[13] S. Cascone, Green Roof Design: State of the Art on Technology and Materials, Sustainability 11 (2019) 3020, https://doi.org/10.3390/su11113020.

[14] M. Shafique, R. Kim, M. Rafiq, Green roof benefits, opportunities and challenges - A review, Renew. Sust. Energ. Rev. 90 (2018) 757-773, https://doi.org/10.1016/j.rser.2018.04.006.

[15] K.L Getter, D.B Rowe, The role of extensive green roofs in sustainable development, Hort Science 41 (5) (2006) 1276-1285, https://doi.org/10.21273/HORTSCI.41.5.1276.

[16] A.L. Congostrina, Azoteas verdes contra el cambio climático. https://elpais.com/espana/catalunya/2020-03-11/azoteas-verdes-contra-el-cambio-climatico.html, 2020 (accessed 12 March 2020).

[17] U. Berardi, A-H. Ghaffarian-Hoseini, A. Ghaffarian Hoseini, State-of-the-art analysis of environmental benefits of green roofs, Appl. Energy 115 (2014) 411-428, https://doi.org/10.1016/j.apenergy.2013.10.047.

[18] B. Baskaran, K. Liu, Thermal performance of green roofs through field evaluation, Proceedings for the First North American Green Roof Infrastructure Conference Awards and Trade Show, 2003.

[19] Green Roofs for Healthy Cities, 2018 Annual Green Roof Industry Survey. http://www.greenroofs.org/, 2019 (accessed 13 April 2021).

[20] A. Sánchez-Ostiz, Cerramientos de edificios: Cubiertas, CIE Inversiones Editoriales DOSSAT 2000, Madrid (Spain), 2003.

[21] Colegio Oficial de Ingenieros técnicos agrícolas y peritos agrícolas de Catalunya, Normas Tecnológicas de Jardinería y Paisajismo - Cubiertas verdes NTJ 11C, Barcelona: s.n, 2012.

[22] Colegio Oficial de Ingenieros técnicos agrícolas y peritos agrícolas de Catalunya, Normas Tecnológicas de Jardinería y Paisajismo- Cubiertas Ecológicas extensivas NTJ 11E, Barcelona: s.n, 1999.

[23] Colegio Oficial de Ingenieros técnicos agrícolas y peritos agrícolas de Catalunya, Normas Tecnológicas de Jardinería y Paisajismo - Cubiertas Ecológicas intensivas NTJ 11I, Barcelona: s.n, 2000.

[24] T. Susca, Green roofs to reduce building energy use? A review on key structural factors of green roofs and their effects on urban climate, Build. Environ. 162 (2019) 106273, https://doi.org/10.1016/j.buildenv.2019.106273.

[25] B.-S. Lin, C.-C. Yu, A.-T. Su, Y.-J. Lin, Impact of climatic conditions on the thermal effectiveness of an extensive green roof. Build. Environ. 67 (2013) 26-33, https://doi.org/10.1016/j.buildenv.2013.04.026.

[26] A. Lemos Galíndez, Análisis teórico-experimental de la resiliencia de cubiertas verdes frente a varios efectos derivados del cambio climático [Tesis Fin de Máster]. España, Santander: Universidad de Cantabria, 2018.

[27] C.Y. Jim, Green roof evolution through exemplars: Germinal prototypes to modern variants. Sust. Cities Soc. 35 (2017) 69-82, https://doi.org/10.1016/j.scs.2017.08.001.

[28] M. Bostenaru Dan, Concise and informative title: innovative geotextile materials for the extension of urban green space - contribution to urban sustainability. Environmental Science Biotechnology 13 (2014) 5-9, https://doi.org/10.1007/s11157-013-9328-9.

[29] S. Bozorg Chenani, S. Lehvävirta, T. Häkkinen, Life cycle assessment of layers of green roofs. J. Clean Prod. 90 (2015) 153-162. https://doi.org/10.1016/j.jclepro.2014.11.070.

[30] Industrial Fabrics Association International Narejo, Green roof market growth: Opportunities and challenges, Geosynthetics 28 (5) (2006) 35-43.

[31] G. Peri, M. Traverso, M. Finkbeiner, G. Rizzo, Embedding “substrate” in environmental assessment of green roofs life cycle: evidences from an application to the whole chain in a Mediterranean site, J. Clean Prod. 35 (2012) 274-287, https://doi.org/10.1016/j.jclepro.2012.05.038.

[32] United Nations, Sustainable development Goals. https://sustainabledevelopment.un.org/sdgs, 2015 (accessed 12 April 2021).

[33] S. Guzmán-Sánchez, D. Jato-Espino, I. Lombillo, J.M. Manuel Diaz-Sarachaga, Assessment of the contributions of different flat roof types to achieving sustainable development, Build. Environ. 141 (2018) 182-192, https://doi.org/10.1016/j.buildenv.2018.05.063.

[34] G.P. Hammond, C.I. Jones, Embodied energy and carbon in construction materials, Proc. Inst. Civ. Eng. - Energy 161 (2008) 87-98, https://doi.org/10.1680/ener.2008.161.2.87.

[35] C.J. Molineux, A.C. Gange, S.P. Connop, D.J. Newport, Using recycled aggregates in green roof substrates for plant diversity, Ecol. Eng. 82 (2015) 596-604, https://doi.org/10.1016/j.ecoleng.2015.05.036.

[36] A.J. Bates, J.P. Sadler, R.B. Greswell, R. Mackay, Effects of recycled aggregate growth substrate on green roof vegetation development: A six year experiment, Landsc. Urban Plan. 135 (2015) 22-31, https://doi.org/10.1016/j.landurbplan.2014.11.010.

[37] S.B. Mickovski, K. Buss, B.M. McKenzie, B. Sökmener, Laboratory study on the potential use of recycled inert construction waste material in the substrate mix for extensive green roofs, Ecol. Eng. 61 (Part C) (2013) 706-714, http://dx.doi.org/10.1016/j.ecoleng.2013.02.015.

[38] J. Mentens, D. Raes, M. Hermy, Green roofs as a tool for solving the rainwater runoff problem in the urbanized 21st century? Landsc. Urban Plan. 77 (3) (2006) 217-226, http://dx.doi.org/10.1016/j.landurbplan.2005.02.010.

[39] B.G. Gregoire, J.C. Clausen, Effect of a modular extensive green roof on stormwater runoff and water quality, Ecol. Eng. 37 (6) (2011) 963-969, https://doi.org/10.1016/j.ecoleng.2011.02.004.

[40] K.L. Getter, D.B. Rowe, G.P. Robertson, B.M. Cregg, J.A. Andresen, Carbon sequestration potential of extensive green roofs, Environ. Sci. Technol. 43 (2009) 7564-7570, http://dx.doi.org/10.1021/es901539x.

[41] J.C. DeNardo, A.R. Jarrett, H.B. Manbeck, D.J. Beattie, R.D. Berghage, Stormwater mitigation and surface temperature reduction by green roofs, Trans. Am. Soc. Civ. Eng. 48 (4) (2005) 1491-1496, https://doi.org/10.13031/2013.19181.

[42] M. Connelly, M. Hodgson, Sound transmission loss of extensive green roofs - Field test results, Can. Acoust. 36 (3) (2008) 74-75.

[43] S. Cascone, A. Gagliano, T. Poli, G. Sciuto, Thermal performance assessment of extensive green roofs investigating realistic vegetation-substrate configurations, 12 Build Simul (2019) 379-393, https://doi.org/10.1007/s12273-018-0488-y.

[44] M. Eksi, D.B. Rowe, R. Fernández-ca, B.M. Cregg, Effect of substrate compost percentage on green roof vegetable production, Urban For. Urban Green. 14 (2015) 315–322, https://doi.org/10.1016/j.ufug.2015.03.006.

[45] M. Turco, G. Brunetti, S.A. Palermo, G. Capano, G. Grossi, M. Maiolo, P. Piro, On the environmental benefits of a permeable pavement: metals potential removal efficiency and Life Cycle Assessment, Urban Water J. 17 (2020) 619-627, https://doi.org/10.1080/1573062X.2020.1713380.

[46] C. Gargari, C. Bibbiani, F. Fantozzi, and C. A. Campiotti, Environmental Impact of Green Roofing: The Contribute of a Green Roof to the Sustainable Use of Natural Resources in a Life Cycle Approach, Agriculture and Agricultural Science Procedia 8 (2016) 646-656, https://doi.org/10.1016/j.aaspro.2016.02.087.

[47] G. Kokogiannakis, J. Darkwa, K. Yuan, A combined experimental and simulation method for appraising the energy performance of green roofs in Ningbo's Chinese climate, Build Simul 7 (2014) 13-20, https://doi.org/10.1007/s12273-013-0149-0.

[48] U. Berardi, The outdoor microclimate benefits and energy saving resulting from green roofs retrofits, Energy Build 121 (2016) 217-229, https://doi.org/10.1016/j.enbuild.2016.03.021.

[49] P. Bevilacqua, D. Mazzeo, N. Arcuri, Thermal inertia assessment of an experimental extensive green roof in summer conditions, Build. Environ. 131 (2018) 264–276, https://doi.org/10.1016/j.buildenv.2017.11.033.

[50] D. Zirkelbach, S.R. Mehra, K.P. Sedlbauer, H.M. Künzel, B. Stockl, A hygrothermal green roof model to simulate moisture and energy performance of building components, Energy Build 145 (2017) 79-91, https://doi.org/10.1016/j.enbuild.2017.04.001.

[51] M. D’Orazio, C. Di Perna, E. Di Giuseppe, Green roof yearly performance: a case study in a highly insulated building under temperate climate, Energy Build 55 (2012) 439-451, https://doi.org/10.1016/j.enbuild.2012.09.009.

[52] K.L. Getter, D.B. Rowe, J.A. Andresen, I.S. Wichman, Seasonal heat flux properties of an extensive green roof in a Midwestern U.S. climate. Energy Build 43 (2011) 3548-3557, https://doi.org/10.1016/j.enbuild.2011.09.018.

[53] J.T. Lundholm, B.M. Weddle, J.S. Macivor, Snow depth and vegetation type affect green roof thermal performance in winter, Energy Build 84 (2014) 299-307, https://doi.org/10.1016/j.enbuild.2014.07.093.

[54] M. Eksi, D.B. Rowe, I.S. Wichman, J.A. Andresen, Effect of substrate depth, vegetation type, and season on green roof thermal properties. Energy Build 145 (2017) 174-187. https://doi.org/10.1016/j.enbuild.2017.04.017.

[55] H.F. Castleton, V. Stovin, S.B.M. Beck, J.B. Davison, Green roofs; building energy savings and the potential for retrofit, Energy Build. 42 (2010) 1582-1591, https://doi.org/10.1016/j.enbuild.2010.05.004.

[56] O. Saadatian, K. Sopian, E. Salleh, C.H. Lim, S. Riffat, E. Saadatian, A. Toudeshki, M.Y. Sulaiman, A review of energy aspects of green roofs. Renew. Sustain. Energy Rev. 23 (2013) 155–168, https://doi.org/10.1016/j.rser.2013.02.022.

[57] D. Jato-Espino, E. Castillo-López, J. Rodríguez-Hernández, J.C. Canteras-Jordana, A review of application of multi-criteria decision making methods in construction, Autom. Constr. 45 (2014) 151-162, https://doi.org/10.1016/j.autcon.2014.05.013.

[58] R. Bernard, Classement et choix en présence de points de vue multiples, La Revue Française d'Informatique et de Recherche Opérationelle 2 (75) (1968) 57.

[59] O. Savadogo, A. Shanian, A non-compensatory compromised solution for material selection of bipolar plates for polymer electrolyte membrane fuel cell (PEMFC) using ELECTRE IV, *Electrochimica Acta* 51 (25) (2006) 5307-5315.

[60] C. Díez Olea,. Estudio de alternativas para hacer frente a problemas de contaminación acústica. Aplicación a varios casos prácticos en Los Corrales de Buelna [Tesis Fin de Máster]. España, Santander: Universidad de Cantabria, 2019.

[61] MITMA, Guía Metodológica para los sistemas de Auditoría, Certificación o Acreditación de la Calidad y Sostenibilidad en el Medio Urbano, s.l.: s.n. 2017.

[62] P. Ahi, C. Searcy, Assessing sustainability in the supply chain: A triple bottom line approach, Appl. Math. Model. 39 (10-11) (2015) 2882-2896, https://doi.org/10.1016/j.apm.2014.10.055.

[63] A. Alves Fernandes, H.E. Prieto Martínez, D.J Henriques da Silva, J. Geraldo Barbosa, Produção de mudas de tomateiro por meio de estacas enraizadas em hidroponia, Pesq. agropec. bras. 39 (4) (2004) 343-348, https://doi.org/10.1590/S0100-204X2004000400007.

[64] Laterlite. https://www.laterlite.es/, 2020 (accessed 29 February 2020).

[65] Projar. https://www.projar.es/, 2020 (accessed 29 February 2020).

[66] ZinCo- Life on roofs, https://zinco-cubiertas-ecologicas.es/. Available at: https://zinco-cubiertas-ecologicas.es/preguntas_frecuentes/sustrato.php, 2020 (accessed 27 February 2020).

[67] N. Tziampou, S.J.Coupe, L.A. Sañudo-Fontaneda, A.P. Newman, D. Castro-Fresno, Fluid transport within permeable pavement systems: A review of evaporation processes, moisture loss measurement and the current state of knowledge, Constr. Build. Mater. 243 (2020) 118179.

[68] N. Tziampou, Evaluation of an open-cell phenolic foam as a water barrier system for permeable pavement systems to control stormwater [PhD thesis]. Spain, Santander: University of Cantabria, 2019.

[69] Placo Saint-Gobain, s.f. Available at: https://www.placo.es/bases-de-datos-de-precios y http://www.generadordeprecios.info/obra_nueva/Fachadas_y_particiones/Entramados_autoportantes/De_placas_de_yeso_laminado/FBY050_Entramado_autoportante_de_placas_de.html#gsc.tab=0 (accessed August 2020).

[70] AENOR, CEN. UNE-EN ISO 14044:2006, Environmental management - Life cycle assessment - Requirements and guidelines.

[71] Standard Methods for the Examination of Water and Wastewater, 2012. *2540 SOLIDS.* 22 ed. s.l.:s.n.

[72] AENOR, CEN. UNE-EN ISO 6946:2021, Building components and building elements - Thermal resistance and thermal transmittance - Calculation methods.

[73] ISO 554:1976. Standard atmospheres for conditioning and/or testing - Specifications.

[74] AENOR, CEN. UNE-EN ISO 11058:2020, Geotextiles and geotextile-related products - Determination of water permeability characteristics normal to the plane, without load.

[75] AENOR, CEN. UNE-EN ISO 12236:2007, Geosynthetics - Static puncture test (CBR test).

[76] AENOR, CEN. UNE-EN ISO 13433:2007, Geosynthetics - Dynamic perforation test (cone drop test).

[77] AENOR, CEN. UNE-EN ISO 12956:2020, Geotextiles and geotextile-related products - Determination of the characteristic opening size.

[78] AENOR, CEN. UNE-EN 12447:2002, Geotextiles and geotextile-related products - Screening test method for determining the resistance to hydrolysis in water.

[79] AENOR, CEN. UNE-EN ISO 13438:2020, Geosynthetics - Screening test method for determining the resistance of geotextiles and geotextile-related products to oxidation.

[80] AENOR, CEN. UNE-EN ISO 9864:2005, Geosynthetics - Test method for the determination of mass per unit area of geotextiles and geotextile-related products.

[81] European Commission - Joint Research Centre - Institute for Environment and Sustainability, 2010. International Reference Life Cycle Data System (ILCD) Handbook - General guide for Life Cycle Assessment. I ed. Luxembourg: Publications Office of the European Union.

[82] J. Coma, A. de Gracia, M. Chàfer, G. Pérez, L.F. Cabeza. Thermal characterization of different substrates under dried conditions for extensive green roofs, Energy Build. 144 (2017) 175-180. https://doi.org/10.1016/j.enbuild.2017.03.031.

[83] A. Pianella, R.E.Clarke, N.S.G. Williams, Z. Chen, L. Aye, Steady-state and transient thermal measurements of green roof substrates, Energy Build. 131 (1) (2016) 123-131, https://doi.org/10.1016/j.enbuild.2016.09.024.

[84] D.J. Sailor, D. Hutchinson, L. Bokovoy, Thermal property measurements for ecoroof soils common in the western U.S., Energy Build. 40 (7) (2008) 1246-1251, https://doi.org/10.1016/j.enbuild.2007.11.004.

[85] Scheirs, J. & Priddy, D. Modern Styrenic Polymers. s.l.:Wiley. 2003.

[86] AENOR, CEN. UNE-EN ISO 11664-6:2017, Colorimetry - Part 6: CIEDE2000 Colour-difference formula.

ASSESSMENT OF DIFFERENT COMBINATIONS OF SUBSTRATE-FILTER MEMBRANE IN GREEN ROOFS

Diego Carrera[a], Ignacio Lombillo[b*], Jaime Carpio-García[c], Haydee Blanco[b]

[a] University of Cantabria, Civil Engineering School, Santander, 39005, Spain

[b] Dept. of Structural and Mechanical Engineering, University of Cantabria, Civil Engineering School, Santander, 39005, Spain

[c] GITECO Research Group, University of Cantabria, Civil Engineering School, Santander, 39005, Spain

HIGHLIGHTS

A methodology to evaluate the substrate layer and the geotextile was designed

Three types of substrates and three geotextiles were analysed

Geotextiles and substrates were combined and nine composite sections were studied

The list of indicators was based on the three pillars of sustainability

Among other solutions, a novel one, based on recycled phenolic foam, was studied

Composite sections including reused or recycled material show higher performance

Declaration of interests

☒ The authors declare that they have no known competing financial interests or personal relationships that could have appeared to influence the work reported in this paper.

☐The authors declare the following financial interests/personal relationships which may be considered as potential competing interests: